

THE EFFECTS OF GROWTH DIFFERENTIATION FACTOR 11 ON
PATHOLOGICAL CARDIAC HYPERTROPHY

A Dissertation
Submitted to
the Temple University Graduate Board

In Partial Fulfillment
of the Requirements for the Degree
DOCTOR OF PHILOSOPHY

by
Shavonn C. Harper
May 2018

Examining Committee Members:

Steven R. Houser, PhD, Advisory Chair, Cardiovascular Research Center
Michael Autieri, PhD, Cardiovascular Research Center
Sadia Mohsin, PhD, Cardiovascular Research Center
Walter J. Koch, PhD, Center for Translational Medicine
Michael Franti, PhD, External Member, Research Beyond Borders; Boehringer-
Ingelheim Pharmaceuticals

ABSTRACT

Pathological cardiac hypertrophy (PCH) occurs in response to pathological stimuli affecting the heart such as coronary artery disease, myocardial infarction, or hypertension. PCH is also be independent risk factor for cardiac events and/or sudden death. Despite therapeutic advancements in the treatment of cardiovascular diseases (CVD) and heart failure, deaths due to CVD remain the leading cause of mortality worldwide. Furthermore, treatment of these cardiovascular diseases slows their progression, but individuals eventually progress to heart failure, which has a 5-year survival rate of approximately 50 percent. There is a clear need for development of new therapies that can reverse PCH and the associated damage to the heart.

As healthcare improves, populations are living longer, and illness due to age increases. One issue that occurs with aging is loss of normal cardiac function leading to heart failure. This functional decline is accompanied by morphological changes in the heart, including hypertrophy. Although it is well documented that myocardial remodeling occurs with aging, the mechanisms underlying these changes are poorly understood.

Growth differentiation factor 11 (GDF11) is a member of the transforming growth factor β (TGF- β) superfamily of proteins, which regulate a number of cellular processes. Shared circulation of a young mouse with an old mouse or a single daily intraperitoneal (IP) injection of GDF11 for 30 days was shown to reverse aging-induced pathological cardiac hypertrophy. This molecule is highly homologous with another TGF- β family member, myostatin, which is a known negative growth regulator of skeletal muscle. We began by attempting to validate published data claiming that a single daily intraperitoneal (IP) injection of 0.1 mg/kg/day of GDF11 could reverse aging induced cardiac

hypertrophy. We performed a blinded study during which treated 24-month-old C57BL/6 male mice with a single IP injection of 0.1 mg/kg/day of GDF11 for 28 days and monitored changes in cardiac function and structure using echocardiography (ECHO). We also looked for differences in fibrosis, myocyte size, markers of pathological hypertrophy and heart weight. We were unable to find any differences between vehicle treated age mice and GDF11 treated aged mice in any of the measured parameters. While we did find an increase in heart weight between 8-week-old mice and the 24-month-old mice, there was no difference in the heart weight to body weight ratios of these groups of animals. From these data we concluded that our aged- mice did not have pathological hypertrophy and the dose of GDF11 used in this study did not have any effect on cardiac structure or function.

Hypertensive heart disease results in changes in cardiac structure and function including left ventricular hypertrophy, systolic and/or diastolic dysfunction. It is also a leading cause of heart failure. Members of the TGF- β superfamily of proteins have been shown to be involved in many of the processes that occur in the heart in response to hypertension, such as the fibrotic response. Although it was previously shown that treatment with 0.1 mg/kg of GDF11 did not prevent pressure overload induced cardiac hypertrophy, we found this dose was too low to alter cardiac structure in our aging study. In addition, a single GDF11 dose is insufficient to fully address this issue. We therefore performed a blinded dose-ranging study to investigate the effects of GDF11 on pressure overload induced cardiac hypertrophy using transverse aortic constriction (TAC) which mimics the effects of chronic hypertension on the heart. In this study, animals received TAC surgery and were assigned to treatment groups so that there were no differences in wall thickness, cardiac function, or pressure gradients across the aortic constriction at the

start of the treatments 1 week after TAC. Mice were given 0.5 mg/kg/day of GDF11, 1.0 mg/kg/day GDF11, 5.0 mg/kg/day of GDF11, or vehicle via a single daily IP injection for 14 days. Using these higher doses, we found that GDF11 had dose dependent effects on both cardiac structure and function following TAC. Myocyte cross sectional area was dose-dependently decreased compared to vehicle treated mice in both sham and TAC conditions. Cardiac function was preserved in the 1.0 and 5.0 mg/kg groups treatment groups after TAC. Left ventricular internal chamber dimensions were preserved with the 1.0 mg/kg treatment group. Treatment with GDF11 caused a dose dependent decrease on both body weight and heart weight in both normal and TAC mice, but with an effect on heart weight in the TAC mice that was independent of body weight. However, the 5.0 mg/kg dose caused large reductions in body weight (cachexia) and death. Our results show that GDF11 can reduce pathological hypertrophy and cardiac remodeling after pressure overload, but there is a narrow therapeutic range.

DEDICATION

This dissertation is dedicated to my family who's love and support made this possible.

ACKNOWLEDGMENTS

Nearly eight years ago, while completing a summer research program at the Marine Biological Laboratories in Woods Hole, Massachusetts, the program directors told us that you must be absolutely sure that you want to complete a PhD because it's one of the hardest challenges you will face should you pursue it. If you don't need a PhD for your career goals, you should not take the time to obtain one. Pursue a master's degree instead. Their statements have held true; there have been many times where I not so jokingly said I wanted to quit. Nevertheless, I have pushed through and have reached the end of my Ph.D. studies. I have a strong support system that has helped me reach this stage in my career and I would now like to thank them.

I must start by thanking my thesis advisor and mentor Dr. Steven Houser. His guidance and support have turned me into the scientist I am today. He provides a light-hearted environment in which we can joke around and be ourselves, yet he inspires us to work hard and fosters our abilities as independent scientists. Thank you, Dr. Houser, for taking me under your wing and helping me to succeed in your laboratory. It has been an amazing 5 years.

This work could not have been completed without the feedback and support of my thesis advising committee: Dr. Michael Autieri, Dr. Walter Koch, Dr. Sadia Mohsin, and Dr. Joseph Rabinowitz. We met every 6 months to discuss my progress, and the feedback you provided was essential in helping to direct and focus the project. You have also provided your time and guidance whenever I needed it. Thank you for everything you have done for me over the years.

I would like to thank my collaborators at Boehringer-Ingelheim as well. They are the reason we initially pursued this project involving GDF11. Without them having reached out to us, we would not have begun studying GDF11. A special thank you goes to Dr. Michael Franti for agreeing to serve as my external member on my committee. You were a part of the project all along and have contributed to the work immensely. Your knowledge in this area of work has been indispensable, and I appreciate the time and effort you put into the completion of this project.

I would also like to thank every member of the Houser lab past and present that I have worked with over the years. Each of them has provided me with guidance and/or friendship during our time together in the lab. From the members that were there when I first started who taught me new techniques and made me feel welcome and comfortable as an incoming member amongst people who had already built strong friendships, to the new members who arrived after I'd been there for years, thank you all. Working beside you was a great experience.

I also need to thank three very special women in my life each of whom influenced my decision to pursue a PhD. The first is my aunt, Evelin Taylor. She has been like a mother to me for my entire life. She always believed in me, pushed me to do my best, and instilled in me the value of a quality education. My education was always a priority to my aunt. I'm very thankful for the role she played in my life. Next, I would like to thank my academic advisors at Ursinus College, Dr. Beth Bailey and Dr. Sheryl Goodman. Dr. Bailey introduced me to cardiac research. Without the influence of these two women while deciding the career path I wanted to pursue, I would not have chosen to pursue a PhD.

To the rest of my family and my friends, I want to thank you for keeping me sane over the last six years. Your support, love, and friendship has kept me going.

Finally, I want to thank my amazing husband, James Harper. Over the past few years he has been my primary support system outside of the lab. He has no background in biological science, but he patiently listens and remembers the things I say about my project and is always there if I need to vent my frustrations of the day. Thank you for always supporting me.

TABLE OF CONTENTS

	Page
ABSTRACT.....	ii
DEDICATION	v
ACKNOWLEDGMENTS	vi
LIST OF TABLES	xiii
LIST OF FIGURES	xiv
LIST OF ABBREVIATIONS	xv
CHAPTER	
1. INTRODUCTION	1
Cardiac Hypertrophy.....	1
Significance.....	1
Types of Cardiac Hypertrophy.....	2
Functional and Structural Changes During Cardiac Hypertrophy	4
Mechanisms of Cardiac Hypertrophy	5
Calcineurin-NFAT Signaling.....	5
G-Protein Coupled Receptors	6
Renin-Angiotensin System	6
Mitogen Activated Protein Kinases	7
TGF β Superfamily of Proteins.....	7
Background	7
TGF β and Smad Signaling in Hypertrophy	8

TGF β and Smad Signaling in Fibrosis.....	9
GDF11 and Myostatin in the Heart	10
Summary and Objectives	12
2. GDF11 IN AGING INDUCED CARDIAC HYPERTROPHY	14
Abstract	14
Rationale	14
Objective.....	14
Methods and Results.....	14
Conclusions	15
Introduction	15
Methods	17
Animals	17
Functional Characterization of GDF11.....	17
GDF11 Dosing and Injections	18
Circulating Levels of GDF11	18
Western Blot Analysis	19
Echocardiography	20
In Vivo LV Pressure Measurements	20
Tissue Processing, Histology, Heart Weight to Body Weight Ratio (HW/BW), Myocardial Fibrosis, and Myocyte Cross Sectional Area.....	20
In-Vitro Fibrosis Assay.....	21
Real-Time Polymerase Chain Reaction (PCR)	22

In Vitro Cardiac Myocyte Hypertrophy Assay	23
Statistics	24
Results	24
Recombinant GDF11 Is Functional and Can Be Selectively and Reliably Detected	24
GDF11 Blood Levels Increase After Injection of rGDF11	26
GDF11 Has No Effect on Cardiac Hypertrophy	26
GDF11 Has No Effect on Cardiac Function	29
GDF11 Did Not Prevent Phenylephrine-Induced Hypertrophy In Vitro	33
Discussion	33
3. GDF11 IN PRESSURE OVERLOAD INDUCED CARDIAC HYPERTROPHY	38
Abstract	38
Rationale	38
Objective	38
Methods and Results	38
Conclusions	39
Introduction	39
Methods	42
Animals	42
Animal Model of Cardiac Hypertrophy	42
GDF11 Dosing and Injections	43

Echocardiography	43
Circulating levels of GDF11	44
Histology, Weight Measurements, Myocardial Fibrosis, and Myocyte Cross Sectional Area.....	45
Western-Blot Analysis	46
Real-Time Polymerase Chain Reaction (PCR)	46
Statistics	48
Results	48
GDF11 Causes Dose Dependent Activation of SMAD2 Signaling	48
GDF11 Decreases TAC-Induced Cardiac Hypertrophy	50
GDF11 Improves Cardiac Function.....	57
GDF11 Decreased Cardiac Fibrosis	57
High Doses of rGDF11 Cause Cachexia	60
Discussion	62
GDF11 Reduces PCH and Improves Cardiac Structure and Function	64
GDF11 Reduces TAC-Induced Interstitial Fibrosis	66
High GDF11 Treatment Doses Cause Cachexia and Death	67
4. CONCLUSIONS AND FUTURE DIRECTIONS.....	69
BIBLIOGRAPHY.....	73

LIST OF TABLES

Table	Page
1. Mouse primer sequences for RT-PCR.....	23
2. Rat primer sequences for RT-PCR	23
3. Circulating levels of GDF11 after injection	27
4. Primer sequences for RT-PCR	47
5. Terminal weights	53
6. Body weights and percent body weight change.....	60

LIST OF FIGURES

Figure	Page
1. Assessment of antibody reactivity and function of rGDF11.....	25
2. Assessment of hypertrophy in-vivo	28
3. Analysis of cardiac fibrosis	30
4. Cardiac structure and function measured by echocardiography	31
5. Intra-left ventricular pressures	32
6. GDF11 induces hypertrophy in NRVMs	33
7. Injections of rGDF11 increase the circulating concentration of GDF11 and SMAD2 phosphorylation	49
8. rGDF11 reduces TAC-induced cardiac hypertrophy	51
9. rGDF11 decreases myocyte cross-sectional area and alters expression of markers of hypertrophy.....	52
10. rGDF11 altered cardiac remodeling after TAC.....	54
11. Schematic of experimental protocol.....	56
12. rGDF11 improves cardiac function after TAC	58
13. rGDF11 reduces interstitial fibrosis and collagen mRNA expression.....	59
14. rGDF11 induces severe cachexia at high dosage.....	61
15. Representative M-mode echocardiograms.....	62

LIST OF ABBREVIATIONS

ACTA1	alpha skeletal actin
α MHC	α -myosin heavy chain
ANP	Atrial natriuretic peptide
β MHC	β -myosin heavy chain
BNP	Brain natriuretic peptide
BW	Body weight
CSA	Cross sectional area
CVD	Cardiovascular Disease
ECHO	Echocardiography
EDP	End diastolic pressure
EF	Ejection fraction
ESV	End systolic pressure
FS	Fractional shortening
Gast	Gastrocnemius
GDF11	Growth differentiation factor 11
HF	Heart failure
HW	Heart weight
IHD	Ischemic heart disease
IP	Intraperitoneal injection
JNK	c-Jun N-terminal kinase
LVAW	Left ventricular anterior wall
LVID	Left ventricular internal dimension
LVPW	Left ventricular posterior wall
NRVM	Neonatal rat ventricular myocyte
PCH	Pathological cardiac hypertrophy
Quad	Quadriceps
RT-PCR	Real time polymerase chain reaction
TA	Tibialis anterior

TAC	Transverse aortic constriction
TGF β	Transforming Growth Factor β
TL	Tibia length
Tric	Triceps
WGA	Wheat Germ Agglutinin

CHAPTER 1

INTRODUCTION

Cardiac Hypertrophy

Significance of Cardiac Hypertrophy

Cardiovascular disease (CVD) is a worldwide epidemic, resulting in the deaths of more than 17 million individuals each year (Joseph et al., 2017). The heart is responsible for pumping blood throughout the circulatory system, thereby providing the other organs and tissues within the body with the oxygen and nutrients necessary for them to function. Cardiac injuries or cardiovascular diseases, such as myocardial infarction, diabetic cardiomyopathy, and hypertension, can result in decreased functioning of the heart and ultimately lead to heart failure (Francis, 2001). Heart failure is a clinical syndrome characterized by low cardiac output resulting from systolic and/or diastolic dysfunction (Drazner, 2011; Lips, deWindt, van Kraaij, & Doevendans, 2003). Within the United States, 5.8 million Americans have heart failure with more than 500,000 new patients diagnosed each year (Roger, 2013). Currently, the 5-year survival rate of heart failure is approximately 50 percent, and the economic burden to the United States is 100 billion U.S. dollars per year (Haldeman, Croft, Giles, & Rashidee, 1999; Malek, 1999; Zannad et al., 1999). The direct medical costs of CVD in the United States is predicted to exceed 800 billion dollars by 2030, with indirect costs increasing 61% to 276 billion dollars. (Heidenreich et al., 2011). Cases of heart failure and deaths resulting from cardiovascular disease are expected to increase despite therapeutic advancements (Benjamin et al., 2017).

Ninety-five percent of all CVD deaths are caused by 6 primary conditions: ischemic heart disease, stroke, hypertensive heart disease, cardiomyopathy, rheumatic

heart disease, and atrial fibrillation (Roth et al., 2015). Many cardiovascular diseases result in left ventricular cardiac hypertrophy, including hypertensive heart disease and ischemic heart disease (Frey, Katus, Olson, & Hill, 2004). If left untreated, left ventricular cardiac hypertrophy leads to cardiac dysfunction and is an independent risk factor for cardiac events such as myocardial ischemia, congestive heart failure, arrhythmias, and sudden death (Diez, Lopez, Gonzalez, & Querejeta, 2001; Haider, Larson, Benjamin, & Levy, 1998).

Improvements in health care and therapies are allowing people to live longer. However, aging presents a new set of problems within the heart as cardiac remodeling and decreases in cardiac pump function sometimes occur with age (Boengler, Schulz, & Heusch, 2009; Yang, Sreejayan, & Ren, 2005). The incidence of and prevalence of diseases such as hypertension, atherosclerosis increase significantly after age 45 in men and 55 in woman, with the odds of having a chronic CVD, hypertension, or chronic heart failure rising to 50%, 85%, and 20% respectively (Lakatta, 2015). Generally, age-related cardiomyopathy is the result of cardiovascular disease, yet age-dependent, disease free changes in cardiac muscle in the absence of disease are not well defined.

Types of Cardiac Hypertrophy

Cardiac hypertrophy is the response of the heart to chronic increases in workload. This hypertrophic response can be divided into two classes based on the stimuli: physiological hypertrophy or pathological hypertrophy (Barry, Davidson, & Townsend, 2008). Physiological hypertrophy occurs during pregnancy or with chronic exercise (Kehat & Molkenin, 2010), while pathological hypertrophy results from sustained pressure or volume overload on the heart, such as from hypertension or myocardial infarction.

Enlargement of the heart muscle results from increases in the size of the cardiac myocytes and proliferation of non-myocytes (Balakumar & Jagadeesh, 2010). It has been well established that physiological hypertrophy induces reversible growth characterized by increases in wall thicknesses, myocyte size, and proportional chamber enlargement (Shimizu & Minamino, 2016). During this type of hypertrophy, the heart maintains normal or enhanced function with morphology and normal gene expression (Ooi, Bernardo, & McMullen, 2014). In contrast to this, a heart undergoing pathological hypertrophy experiences fibrosis, activation of the fetal gene program, myocyte apoptosis and necrosis, and inflammation (Frey & Olson, 2003; Ooi et al., 2014; Ying et al., 2009). During the adaptive phase of hypertrophy, the left ventricular walls thicken, the left ventricular chamber dimensions decrease or remain the same, and cardiac function is maintained (Heineke & Molkentin, 2006). If the stimulus is not removed, further remodeling can cause the heart to progress to dilated hypertrophy, which is characterized by left ventricular wall thinning and increased internal chamber dimensions, accompanied by fibrosis, activation of fetal genes, and apoptosis (Berk, Fujiwara, & Lehoux, 2007; X. M. Li et al., 2009).

Pathological cardiac hypertrophy can be classified as concentric or eccentric hypertrophy based on the geometrical changes in the heart as well as changes in the cardiac myocyte (Bernardo, Weeks, Pretorius, & McMullen, 2010). Eccentric hypertrophy generally develops in response to volume overload and refers to an increase in cardiac mass with an increased chamber volume, while concentric hypertrophy occurs in response to pressure overload and refers to an increase in wall thickness and cardiac mass with either a small decrease or no change in chamber volume (Grossman, Jones, & McLaurin, 1975; van Berlo, Maillet, & Molkentin, 2013). During concentric hypertrophy, sarcomeres are

added to the myocyte in parallel, resulting in an increase in the width of the myocyte, while sarcomeres are instead added in series increasing the length of the myocyte to create an eccentric hypertrophic phenotype (Bernardo et al., 2010; Esposito et al., 2002; Nadruz, 2015).

Functional and Structural Changes During Cardiac Hypertrophy

The heart undergoes many changes in response to pathological stimuli that induce hypertrophy. Studies using transverse aortic constriction (TAC) in mice and rats have been used to better understand the changes that occur in the heart due to pressure overload such as that seen in patients with hypertension or aortic stenosis, with a focus on targeting these mechanisms behind these changes. Although the severity of left ventricular remodeling and time frame for the progression to heart failure is dependent on the strain of mouse used, the sex of the mouse used, and the size of the needle used to create the constriction, this model is highly reproducible when conditions are unchanged (Barrick et al., 2009; Rothermel et al., 2005; Skavdahl et al., 2005). These animal studies have shown that TAC causes increased left ventricular pressures, decreases in cardiac function as measured by echocardiography (ECHO), increases in myocyte size, and increases in both interstitial and perivascular fibrosis (Bae et al., 2011; Furihata et al., 2016; Qin et al., 2015). They have also documented increased apoptosis after pressure overload, as well as changes in cardiac metabolism (Kato et al., 2010; X. M. Li et al., 2009; Teiger et al., 1996; L. Zhang et al., 2013). Furthermore, these studies have also highlighted the inflammatory response that occurs during pressure overload. TAC rapidly induces upregulation of inflammatory cytokines such as TNF α and IL-1 β , with expression returning to sham levels within 7 days after TAC (Ying et al., 2009). Other studies have found that mRNA expression levels of

inflammatory mediators peak at 7 days (Kallikourdis et al., 2017). Leukocyte infiltration into the cardiac tissue also occurs within 7 days after TAC but is partially resolved after 28 days of banding (Kai et al., 2006; Ying et al., 2009). Endothelial cell IL-33 has been linked to the resultant systemic inflammation that occurs after pressure overload (Chen, Hong, Gannon, Kakkar, & Lee, 2015).

Mechanisms of Cardiac Hypertrophy

The type of hypertrophy the heart undergoes and the corresponding functional and morphological changes that accompany it are dependent on the stimuli, as different stimuli activate different intracellular signaling pathways. The two major stimuli for pathological hypertrophy are mechanical stress and neural/hormonal factors (Ritter & Neyses, 2003). Numerous neurohormonal signaling pathways that are activated in response to pathological stimuli have been identified, including the calcineurin-NFAT signaling pathway, G-protein coupled receptors, the renin-angiotensin-aldosterone system, mitogen activated protein kinases signaling, and pathways activated by TGF β . There is cross-talk between these signaling pathways.

Calcineurin-NFAT Signaling

Calcineurin is a calcium/calmodulin dependent protein phosphatase that dephosphorylates the nuclear factor of activated T-cells transcription factors (NFAT) resulting in myocardial hypertrophy (Agrawal, Agrawal, Koyani, & Singh, 2010). In response to pathological stimuli calcineurin dephosphorylates NFAT, which then translocates to the nucleus and activates hypertrophic genes (Bourajjaj et al., 2008; Luedde, Katus, & Frey, 2006). Evidence suggesting a role for calcineurin-NFAT signaling in cardiac hypertrophy can be found in animal studies in which the use of cyclosporine, a

calcineurin inhibitor, inhibited cardiac hypertrophy in animals models of myocardial infarction and pressure overload induced hypertrophy (Meguro et al., 1999; Oie, Bjornerheim, Clausen, & Attramadal, 2000). The activity of calcineurin/NFAT signaling is limited to pathological cardiac hypertrophy (Wilkins et al., 2004).

G-Protein Coupled Receptors

G-Protein coupled receptors (GPCRs) are a conserved family of seven transmembrane receptors. The heterotrimeric G protein complex is comprised of a $G\alpha$ subunit, consisting of four main families ($G\alpha_s$, $G\alpha_{i/o}$, $G\alpha_{q/11}$ and $G\alpha_{12/13}$) coupled to a combination of $G\beta$ (5 members) and $G\gamma$ (12 members) subunits (Tilley, 2011). G-proteins and their coupled receptors serve many functions within the heart in both healthy and diseased states. Receptors coupled to $G\alpha_q$ have been shown to play important roles in mediating cardiac growth responses, myocyte apoptosis, and cardiac hypertrophy (Salazar, Chen, & Rockman, 2007). Blocking $G\alpha_q$ signaling using genetically altered mice blunted cardiac hypertrophy after TAC and preserved cardiac function, while wild-type mice in this study experienced progressive LV dilation and cardiac dysfunction (Esposito et al., 2002). Chronic activation of $G\alpha_s$ signaling pathways in mice with cardiac overexpression of $G\alpha_s$ caused increased heart rate and contractility in response to catecholamine stimulation, but eventually resulted in the development of histological evidence of myocardial damage such as cellular hypertrophy, fibrosis, and necrosis (Gaudin et al., 1995; Iwase et al., 1996).

Renin-Angiotensin System

The renin-angiotensin system (RAS) is a hormonal system responsible for regulating blood pressure and blood volume (Cowan & Young, 2009). Angiotensin II is the primary mediator of the physiological actions of RAS (Agrawal et al., 2010). It has

been shown to promote cardiac hypertrophy in vitro (Mehta & Griendling, 2007). Angiotensin II causes ventricular hypertrophy independently of its effect on blood pressure via the angiotensin 1 receptor (P. Lijnen & Petrov, 1999). Blockade of the RAS system by inhibitors of angiotensin converting enzyme (ACE) or angiotensin receptor blockers (ARBs) has been shown to prevent cardiac hypertrophy in animal models of pressure overload (L. Li et al., 2010).

Mitogen Activated Protein Kinases

The mitogen activated protein kinase (MAPK) signaling pathways control numerous cellular functions including transcriptional regulation and apoptosis. These kinases are also important in the modulation of pathological cardiac hypertrophy. The MAPK cascade is subdivided into three main branches which consist of p38 kinases, c-Jun N-terminal kinases (JNKs), and extracellular signal-regulated kinases (ERK1/2) (van Berlo et al., 2013). MAPK signaling is induced in cardiac myocytes by small G-proteins, G-protein coupled receptors, and stress. Constitutive activation of ERK1/2 signaling in the heart through expression of activated MEK1 has been shown to produce concentric hypertrophy without progression to heart failure, while protecting against cell death (Bueno et al., 2000; Lips et al., 2004). Isoproterenol induced cardiac hypertrophy and fibrosis was prevented in mice following gallic acid treatment, and this was associated with decreased phosphorylation of JNK and ERK proteins (Ryu et al., 2016).

TGF β Family Members in Hypertrophy and Fibrosis

Background

The TGF β superfamily of proteins is comprised of more than 30 structurally related proteins that can be subdivided into two major subfamilies of proteins: the bone

morphogenic proteins/growth and differentiation factors and the TGF β /activins (Hata & Chen, 2016). These proteins act as cytokines performing diverse functions throughout the body, including roles in growth, differentiation, and tissue repair (Brand & Schneider, 1995; Massague, 1990). In the canonical signaling pathway for members of this family, ligand binding induces the formation of heterotetramers consisting of two type II and two type I receptors; the constitutively active type II receptor phosphorylates the type I receptor which then phosphorylates the R-Smad leading to its activation (Wrana, 2013). Smads are intracellular signal transducers for the TGF β superfamily which translocate to the nucleus to regulate transcription of target genes (Weiss & Attisano, 2013). Smad proteins are classified into three groups the R-Smads (Smad1, 2, 3, 5 and 8), common-mediator Smads (Co-Smad4), and inhibitory Smads (I-Smad6 and 7) (Pardali & Ten Dijke, 2012). TGF β can also activate other protein kinases and signaling pathways, including Rho family guanosine triphosphatases (GTPases), MAPKs, and protein kinase B/Akt (Attisano & Wrana, 2002). The role of TGF β and Smad2/3 in cardiac hypertrophic and the fibrotic response in the heart has been studied extensively.

TGF β and Smad Signaling in Hypertrophy

It is well established that TGF β mRNA levels are increased in the left ventricular myocardium of patients with hypertrophic cardiomyopathy or idiopathic cardiomyopathy, and protein levels are increased in macrophages and fibroblasts after MI (Edgley, Krum, & Kelly, 2012). When TGF β 1 was inhibited via knockout in a mouse model of chronic angiotensin II induced cardiac hypertrophy, TGF β 1 deficient mice had no significant change in left ventricular mass, cardiomyocytes cross sectional area, and percent fractional

shortening during treatment, while wild-type mice showed a >20% increase in LV mass and impaired cardiac function (Schultz Jel et al., 2002).

Smad3 signaling has been shown to be antihypertrophic. In a mouse model of pressure overload, Smad3 was shown to bind to FBXO32 prior to the activation of Pak 1, and this is crucial for the transcriptional regulation of FBXO32 (Tsui et al., 2015). Loss of Smad3 resulted in a significant increase in cardiac hypertrophy (Divakaran et al., 2009). There is crosstalk between the TGF β family canonical Smad signaling pathways and kinases from other signaling pathways. RSmads contain a serine and proline rich linker region that can also be phosphorylated on Ser or Thr by other kinases, e.g. ERK, MAPK and CDK kinases, which consequently control Smad activities (Hata & Chen, 2016). These kinases (ERK, MAPK) have been implicated in hypertrophy.

TGF β and Smad Signaling in Fibrosis

TGF β activates fibroblasts inducing the expression of extra cellular membrane components, induces transdifferentiation of fibroblasts into myofibroblast, and has a positive feedback effect on its own expression in myocytes and fibroblasts further promoting its own expression (Edgley et al., 2012; P. J. Lijnen, Petrov, & Fagard, 2000). TGF β also enhances extracellular matrix protein synthesis and suppresses the activity of proteases that degrade extracellular matrix by inhibiting MMP expression and by inducing synthesis of protease inhibitors, such as Plasminogen Activator Inhibitor (PAI)-1 and TIMPs (Bujak & Frangogiannis, 2007). Angiotensin II induces overexpression of TGF β 1 mediates cardiac remodeling and hypertrophy in an autocrine and paracrine manner by inducing the proliferation of cardiac fibroblasts and enhancing the deposition of extracellular matrix proteins such as collagen (Schultz Jel et al., 2002; Wenzel,

Taimor, Piper, & Schluter, 2001). Smad signaling has been shown to be profibrotic, with decreases in Smad 3 decreasing cardiac fibrosis in mouse models of pressure overload and agonist induced hypertrophy (Divakaran et al., 2009; Ryu et al., 2016).

GDF11 and Myostatin in the Heart

The actual function of GDF11 in the heart is understudied. However, understanding the proposed roles of another member of the TGF β superfamily, myostatin/GDF8, in the heart may shed some light on the role of GDF11. GDF11 and myostatin are highly homologous, sharing approximately 90% homology. They bind to the same receptor, ActRIIb with similar affinities, and signal through the smad2/3 pathway (Sako et al., 2010). Despite this, myostatin is largely expressed in skeletal muscle, with lower expression in heart and adipose tissue, while GDF11 is expressed in a variety of tissues, including the pancreas, intestine, kidney, skeletal muscle, heart, developing nervous system, olfactory system, and retina (McPherron, 2010). This may suggest slightly different roles for myostatin and GDF11. Myostatin also circulates at much higher concentrations than GDF11, which questions the physiological relevance of circulating levels of GDF11 in adult tissues.

Under pathological injury or stress conditions, such as myocardial infarction or hypertension, myostatin expression in the heart increases (Fernandez-Sola, Borrissier-Pairo, Antunez, & Tobias, 2015; George et al., 2010; Sharma et al., 1999). This increased cardiac myostatin enters the circulation and acts on skeletal muscle leading to atrophy of the skeletal muscle (Castillero et al., 2015; Heineke et al., 2010). However, myostatin also has some effects in cardiac muscle (Breitbart, Auger-Messier, Molkentin, & Heineke, 2011). In a cardiac specific overexpression model, transaortic constriction increased

circulating myostatin level 3-4-fold. These mice had a reduction in heart weight, while myostatin null mice developed increased hypertrophy in response to infusion of the $\alpha 1$ adrenergic receptor agonist, phenylephrine (Heineke et al., 2010). Other groups have likewise shown a role for myostatin in regulating cardiac muscle growth with loss of myostatin increasing hypertrophy and upregulation decreasing cardiac muscle growth (Artaza et al., 2007; Bish, Morine, Sleeper, & Sweeney, 2010; Jackson et al., 2012; Rodgers et al., 2009). Myostatin has been shown to regulate cardiomyocyte growth via modulation of the Akt signaling pathway (Morissette et al., 2006). However, a study investigating the systemic and cardiac effects of myostatin deletion in aged mice (27-30 months old) found that myostatin deletion had no effect on aging-related increases in cardiac mass (Morissette et al., 2009).

Myostatin has also been shown to have protective role against heart failure by stimulating expression of regulator of G-protein signaling 2, a GTPase-activating protein that restricts β -adrenergic and Gq-mediated signaling (Biesemann et al., 2014). These signaling pathways have been linked to heart failure, hypertrophy, decreases in contractility, and sudden cardiac death (Braz et al., 2004; van Oort et al., 2006; T. Zhang et al., 2003). In this study, short-term overexpression improved cardiac contractility and inhibited cardiac hypertrophy, while deletion of myostatin in adult cardiomyocytes led to heart failure and increased lethality (Biesemann et al., 2014).

Some studies that suggest increased myostatin, and potentially GDF11 expression, could be beneficial in the aging heart, but there is another effect of these molecules which is less beneficial. Just as TGF- β promotes cardiac fibrosis, myostatin is capable of inducing cardiac fibrosis. Long-term overexpression of myostatin results in increased interstitial

cardiac fibrosis, while constitutive loss of myostatin protects from cardiac fibrosis during aging (Biesemann et al., 2015; Morissette et al., 2009). Likewise, by 9 months of age, mice overexpressing myostatin develop large patches of fibrotic area composed of interstitial and perivascular fibrosis and develop cardiac dysfunction with significantly decreased ejection fraction and stroke volumes, and increased end systolic and end diastolic volumes as measured by cardiac MRI (Biesemann et al., 2015).

Summary and Objectives

There is substantial evidence in the literature that TGF β family members are involved in the pathways that are activated during cardiac remodeling that accompanies cardiac hypertrophy. A set of publications out of a laboratory in Harvard claimed that GDF11 was an anti-aging protein that was capable of reversing aging induced cardiac hypertrophy, decreasing fibrosis in the aged heart, and reducing fat mass, while preserving lean muscle mass (Loffredo et al., 2013; Poggioli et al., 2016). In the years following this publication, other studies have shown the effects of this molecule in the heart are complex, and there have been mixed results. In addition, it has been established that very high levels of GDF11 result in both skeletal and cardiac muscle cachexia (Hammers et al., 2017; Zimmers et al., 2017). The central question remains the same: does GDF11 play a beneficial role in the heart? The research on myostatin suggests that despite decreasing cardiac mass and preventing heart failure, myostatin expression increases cardiac fibrosis which decreases cardiac function. The proposed beneficial role for GDF11 has not been reproducible, so the effect of this molecule on the heart remains a highly debated subject. More research examining the signaling mechanisms of GDF11 in cardiac tissue needs to be performed to link the proposed anti-hypertrophic effect of GDF11.

The objectives of the current body of research were to 1) determine if and by what mechanism GDF11 reverses aging-induced cardiac hypertrophy and 2) determine the effects of GDF11 on TAC induced cardiac hypertrophy. The hypothesis of this work was that GDF11 can reduce cardiac size and alter cardiac remodeling.

CHAPTER 2

GDF11 IN AGING INDUCED CARDIAC HYPERTROPHY

Abstract

Rationale

GDF11 (Growth Differentiation Factor 11) is a member of the transforming growth factor β (TGF β) super family of secreted factors. A recent study showed that reduced GDF11 blood levels with aging was associated with pathological cardiac hypertrophy (PCH) and restoring GDF11 to normal levels in old mice rescued PCH.

Objective

To determine if and by what mechanism GDF11 rescues aging dependent PCH.

Methods and Results

24-month-old C57BL/6 mice were given a daily injection of either recombinant (r) GDF11 at 0.1mg/kg or vehicle for 28 days. rGDF11 bioactivity was confirmed in-vitro. After treatment, rGDF11 levels were significantly increased but there was no significant effect on either heart weight (HW) or body weight (BW). HW/BW ratios of old mice were not different from 8 or 12-week-old animals, and the PCH marker ANP was not different in young versus old mice. Ejection fraction, internal ventricular dimension, and septal wall thickness were not significantly different between rGDF11 and vehicle treated animals at baseline and remained unchanged at 1, 2 and 4 weeks of treatment. There was no difference in myocyte cross-sectional area rGDF11 versus vehicle-treated old animals. In vitro studies using phenylephrine-treated neonatal rat ventricular myocytes (NRVM), to explore the putative anti-hypertrophic effects of GDF11, showed that GDF11 did not reduce NRVM hypertrophy, but instead induced hypertrophy.

Conclusions

Our studies show that there is no age-related PCH in disease free 24-month-old C57BL/6 mice and that restoring GDF11 in old mice has no effect on cardiac structure or function.

Introduction

Cardiovascular function can decline in old age, and the disease independent factors that induce these changes are not well known. A recent study suggests that disease-free aging induces pathological cardiac hypertrophy (PCH) in 24-month-old mice and that this results in large part from an age-related reduction in the circulating blood levels of Growth Differentiation Factor 11 (GDF11), a member of the Transforming Growth Factor β (TGF β) super family of cytokines (Loffredo et al., 2013). GDF11 and related family members generally reduce skeletal muscle protein synthesis and repair and enhance protein degradation, which leads to muscle atrophy in adults (Kollias & McDermott, 2008; Ohsawa et al., 2012). Loss of these factors, particularly myostatin (also called GDF8) (Mosher et al., 2007; Parsons, Millay, Sargent, McNally, & Molkenin, 2006) is primarily associated with skeletal muscle hypertrophy but with limited effects on the heart (Heineke et al., 2010). Recent work suggests that circulating levels of GDF11 decrease with aging, and restoring a “youthful” circulation containing normal levels of GDF11 to old mice via parabiosis reversed age-dependent pathological cardiac hypertrophy (Loffredo et al., 2013). A major finding of this study was that restoring youthful levels of GDF11 by injecting recombinant (r) GDF11 into old animals restored normal myocyte size and gene expression in the old mouse heart. Related studies suggest that restoring GDF11 can also

have beneficial effects on skeletal muscle (Sinha et al., 2014) and brain function (Katsimpardi et al., 2014), suggesting that restoring GDF11 to levels seen in young animals could reverse critical aspects of age-related brain, skeletal muscle and cardiac dysfunction. These studies suggest that restoring normal GDF11 levels in old age can reverse aging effects on critical organ systems.

The idea that a member of the TGF super family of cytokines, GDF11, is singularly responsible for aging related organ dysfunction is not supported by some recently published reports (Egerman et al., 2015). A study to reexamine the idea that reduced GDF11 in aging is responsible for defective skeletal muscle repair could not confirm most aspects of the studies related to GDF11-induced rescue of skeletal muscle wasting with aging (Egerman et al., 2015). This newest report (Egerman et al., 2015) showed that aging involves skeletal muscle wasting and that increased rather than decreased levels of myostatin and GDF11 are involved. These data suggest that inhibition rather than stimulation of myostatin/GDF11 signaling in aging could blunt the associated skeletal muscle dysfunction.

The goals of the present study were to reexamine the idea that restoring youthful levels of GDF11 in old mice, by injection of rGDF11, reverses pathological cardiac hypertrophy and imparts a “youthful” phenotype to the old heart (Loffredo et al., 2013). If these findings could be confirmed, we then planned to explore what aspects of pathological myocyte function were rescued by rGDF11 treatment.

We performed a blinded study in which we treated 24-month-old C57BL/6 mice with rGDF11 for 28 days, following the protocol used previously (Loffredo et al., 2013). We measured cardiac structure and function before and after rGDF11 treatment and then

measured heart and myocyte size and changes in molecular remodeling after treatment. Our studies suggest that while hearts of older mice are larger there is no pathological hypertrophy present. We also found that daily injection of rGDF11 (Loffredo et al., 2013) significantly raised blood levels of rGDF11 in old mice. However, we did not observe any reduction in heart or myocyte size, nor did we observe any changes in cardiac performance. We also showed that rGDF11 induced hypertrophy in neonatal myocytes and did not block phenylephrine-induced neonatal myocyte hypertrophy (Loffredo et al., 2013).

Methods

Animals

All animal studies were performed according to protocols approved by the Institutional Animal Care and Use Committee of Temple University School of Medicine and conducted in accordance with the *Guide for the Use and Care of Laboratory Animals*. Aged (24 months) C57BL/6 male mice were provided by Boehringer Ingelheim Pharmaceuticals.

Functional Characterization of GDF11

Functional activity of recombinant GDF11 (R&D Systems) was verified before use, by defining its ability to activate Smad2/3 signaling in HepG2 reporter cells. Briefly, HepG2 cells were transfected with Cignal Lentiviral (Qiagen) particles expressing an inducible firefly luciferase reporter under control of Smad2/3-specific TRE (AGCCAGACA). A puromycin-selected stable reporter cell line was used in the experiment as follows. The HepG2 Smad2/3 luciferase reporter cells were harvested, washed and resuspended at a concentration of 1×10^6 cells per ml in Opti-MEM assay

medium. Reporter cells were incubated in a 96-well plate at 50,000 cells per well with serial dilutions of rGDF11. After 24-hour incubation, samples were treated with 100ul STEADY-Glo reagent (Promega), and assayed for luciferase expression. Relative Luminescence Units (RLU) were plotted versus Log₁₀ nano molar concentrations of the test rGDF11, where EC₅₀ & EC₉₀ values were calculated using a 4 Parameter Logistic Model, supported by Excel add-in Xlfit (ID Business Solutions Limited).

GDF11 Dosing and Injections

We followed the protocol used in the previous report(Loffredo et al., 2013). Investigators were blinded to treatment. Animals were given a daily single intraperitoneal injection of either rGDF11 (R&D Systems) at 0.1mg/kg or vehicle (60mM NaAcetate Buffer, pH 5.0 and 10% Trehelose) daily for 28 days. rGDF11 stock solution was dissolved in NaAcetate Buffer, pH 4.5 at a concentration of 1mg/ml. Stock solutions were diluted with the dosing solution (60mM NaAcetate Buffer, pH 5.0 and 10% Trehelose) to reach the final concentration of 0.1mg/kg. Boehringer Ingelheim Pharmaceuticals provided all solutions in a blinded fashion. Animals were weighed every day before dosing.

Circulating Levels of GDF11

rGDF11 and vehicle-treated animals were divided into two groups to determine peak and trough circulating levels of GDF11 in vivo and after injection. Preliminary studies showed that peak GDF11 blood levels were found within 2 hours of injection. Therefore, 1-3 hours before sacrifice, animals were given a final injection of rGDF11 or vehicle to determine the peak plasma levels of GDF11 post injection. Animals in the trough group were sacrificed 24 hours after their final injection. Plasma was collected from blood removed from the left ventricle via cardiac puncture.

Plasma levels of GDF11 were measured using the 2-Step Homebrew Assay Protocol for the Simoa Assay (Quanterix). Assay conditions were as follows: Capture was performed using R&D Systems anti-GDF11 antibody conjugated to paramagnetic beads (0.7mg/ml, 5.0E+06 final bead concentration). Detection was performed using R&D Systems anti-GDF11 antibody labeled with Biotin (60X, final stock 1.8ug/ml). A standard curve was created using R&D Systems rGDF11 in 3% BSA with 0.05% Tween. The Quanterix SBG enzyme was used at a final concentration of 100pM.

Western Blot Analysis

Recombinant human GDF8 (myostatin) and GDF11 were purchased from Peprotech or R&D Systems. 100ng of protein was resolved on 4-12% Bis-Tris mini gels (life technologies) either under non-reducing or reducing conditions with 100mM DTT. Transfer to nitrocellulose membranes was done on an Invitrogen iBlot transfer system. Membranes were blocked for 1hr in 2% BSA (Promega) + 0.05% Tween-20 in Tris Buffered Saline, pH7.5. Primary anti-GDF11 antibodies (R&D Systems or abcam) were used at 1ug/ml diluted in 2%BSA + 0.05% Tween-20 in Tris Buffered Saline, pH7.5, 1hr at room temperature with gentle rocking. Membranes were washed 3 times in 0.05% Tween-20 in Tris Buffered Saline, pH7.5. Secondary antibodies were (for R&D antibody), goat anti-rabbit IgG-HRP (life technologies) or (for abcam antibody), goat anti-rabbit-HRP (life technologies) used at 1:3000 dilution for 1hr at room temperature with gentle rocking. After 3 additional washes, membranes were developed using HRP Chemiluminescent Substrate Reagent Kit (Invitrogen). Images were captured on a Bio-Rad Image Analyzer.

Echocardiography

Anesthetized mice underwent transthoracic echocardiography using a Vevo2100 ultrasound system (VisualSonics; Toronto, Canada). Repeated measurements were performed as previously described (Duran et al., 2012; Taghavi et al., 2012; H. Zhang et al., 2012) at baseline and at 1, 2 and 4 weeks post initial injection. Images were acquired in the short-axis B-mode and M-mode for analysis of cardiac function and dimensions.

In-Vivo LV Pressure Measurements

LV pressures were measured with a 1.4-Fr Millar pressure catheter (SPR-671, Millar Instruments, Houston, TX) connected to an ADInstruments PowerLab 16/30 (ADInstruments, Colorado Springs, CO) with LabChart Pro 6.0 software. Mice were anesthetized with 2.5% isoflurane to maintain HRs in the 450–470 beats/min range, and then a midline neck incision was made and the right carotid artery was exposed and the catheter introduced. The pressure catheter was then advanced through the aortic valves into the LV. The catheter was carefully adjusted to avoid direct contact with the ventricular wall so that smooth intra-LV pressure traces were recorded. Five minutes of baseline pressure were recorded. Intra-LV blood pressure was continuously measured. Pressure data were analyzed offline with the blood pressure module in the LabChart6.0 software.

Tissue Processing, Histology, Heart Weight to Body Weight Ratio (HW/BW), Myocardial Fibrosis and Myocyte Cross Sectional Area

Prior to sacrifice rGDF11 and vehicle treated animals were randomly divided to be used for molecular analysis or histology. Animals were sacrificed 24 hours after their 28th injection. All hearts were rinsed with PBS and weighed. Tibias were removed and measured to the nearest 0.5mm. The hearts from 50% of animals per group were

immediately frozen for molecular analysis. The remaining hearts were perfusion-fixed with 10% formalin and paraffin embedded for histology following previously published protocols (Duran et al., 2013; Duran et al., 2012; Taghavi et al., 2012). Tissue blocks were sent to AML Laboratories (Baltimore, MD) for sectioning and staining for Hemotoxylin and Eosin. Myocyte cross sectional area was measured from 6 animals per group using H and E stained slides. 6 samples from each group were stained with Masson's trichrome (Sigma-Aldrich; St. Louis, MO) for collagen deposition. Myocyte cross-sectional area and Fibrotic area were quantitated with NIH ImageJ software (<http://rsbweb.nih.gov/ij/>). At least 100 myocytes from 4 sections of the heart were analyzed per animal to assess myocyte cross sectional area. 12 fields of view were analyzed per animal for collagen deposition. Fibrotic area was measured by visualizing all blue-stained areas. Color based- thresholding was used to differentiate between the total area of collagen deposition, stained in blue, and myocyte areas in each section. Fibrosis is presented as the sum of the blue-stained areas divided by total ventricular area.

In-Vitro Fibrosis Assay

Normal human dermal fibroblasts (Lonza) were cultured in a 96-well plate at passage 3 to 90% confluence. Cells were serum starved for 24 hours. Cells were treated with a titration of TGF- β 1, GDF-11, or GDF-8 at 1:3 dilutions, or medium control (all proteins purchased from R&D systems) for 48 hours. Cells were fixed in methanol for 30 min at -20°C. Fibronectin was labeled with 1 μ g/ml anti fibronectin goat IgG (Santa Cruz), at ambient temperature for 1hr. Alexa Fluor 555 conjugated anti goat IgG (Life Technologies) was used for secondary labeling, at ambient temperature for 1 hr. Fluorescence intensity at Ex: 555nm and Em: 580nm was determined using a Safire²

microplate reader from Tecan. Fluorescence intensity values are plotted as a percent change from medium control.

Real-Time Polymerase Chain Reaction (RT-PCR)

RNA was extracted from mouse hearts and from rat neonatal cardiomyocytes with TRIzol Reagent. The RNA was cleaned using the Quick-RNA™ MiniPrep (Zymo Research) clean-up protocol. Reverse transcription (RT) reaction was performed using the SuperScript III first strand synthesis system for RT-PCR (Invitrogen) and oligo-dt primers according to the manufacturer's instructions. Real-time PCR was performed using the Quantifast Sybrgreen PCR kit (Qiagen). Data generated from mouse heart samples were normalized to 18SRNA expression, and data generated from rat neonatal cardiomyocytes were normalized to Glyceraldehyde 3-phosphate dehydrogenase (GAPDH) expression. The primer sets used for the mouse and rat samples are listed in tables 1 and 2, respectively.

In-Vitro Cardiac Myocyte Hypertrophy Assay

Neonatal rat cardiac myocytes (NRCMs) were isolated from 1-day old rat pups. NRCMs were plated on coverslips and incubated overnight in DEM+10% FCS (12 well plates and 2x12 plates coverslips). After 24 hours, NRCMs were switched to serum free media (DMEM F12+1xITS). After 2 hours, cells were pretreated with rGDF11 at the following concentrations: 0.5nM, 5nM, and 50nM. Cells were incubated with rGDF11 for 24 hours, before phenylephrine was added at 50 μ M. Cells were incubated for an additional 24 hours for RNA preparation or 48 hours for analysis of cell size and myofibril organization. Cells were washed with cold 1x PBS before being processed for RNA isolation or Fixed with 4% paraformaldehyde.

Table 1: Mouse primer sequences for RT-PCR

Gene	Sequence
18s F	5'- GTAACCCGTTGAACCCCAT
18s R	5'-CCATCCAATCGGTAGTAGCG
atrial natriuretic factor (ANF) F	5'-GCCCTGAGTGAGCAGACTG
atrial natriuretic factor (ANF) R	5'-GGAAGCTGTTGCAGCCTA
brain natriuretic factor (BNP) F	5'-CTGCTGGAGCTGATAAGAGA
brain natriuretic factor (BNP) R	5'-AGTCAGAAACTGGAGTCTCC
alpha myosin heavy chain (α MHC) F	5'-ACCTACCAGACAGAGGAAGA,
alpha myosin heavy chain (α MHC) R	5'-ATTGTGTATTGGCCACAGCG
beta myosin heavy chain (β MHC) F	5'-ACCTACCAGACAGAGGAAGA
beta myosin heavy chain (β MHC) R	5'- TTGCAAAGAGTCCAGGTCTGAG

Table 2: Rat primer sequences for RT-PCR.

Gene	Sequence
GAPDH F	5'- GACATGCCGCCTGGAGAAAC
GAPDH R	5'- AGCCCAGGATGCCCTTTAGT
atrial natriuretic factor (ANF) F	5'- ATCTGATGGATTTCAAGAACC
atrial natriuretic factor (ANF) R	5'- CTCTGAGACGGGTTGACTTC
brain natriuretic factor (BNP) F	5'- ACAATCCACGATGCAGAAGCT
brain natriuretic factor (BNP) R	5'- GGGCCTTGGTCCTTTGAGA

For analysis of myocyte surface area, cells were stained with rabbit anti-troponin I (Cell Signaling) and goat anti-ANP (Santa Cruz). Myocyte surface area was measured for at least 200 cells per condition using NIH ImageJ software.

Statistics

Data are reported as mean \pm standard error of the mean. Unpaired t-test, two-way analysis of variance (ANOVA), or two-way ANOVAs for repeated measures were used to detect statistical significance with GraphPad Prism 6. All cell measurements from the same heart were averaged as one averaged data point. At least three hearts from each group were studied.

Results

Recombinant GDF11 is Functional and Can Be Selectively and Reliably Detected

Using Western analysis, we first tested the specificity of the reagents used in the previous study (Abcam anti-GDF11) to document reduced GDF11 with aging and reductions in cardiac hypertrophy after rGDF11 injections (Loffredo et al., 2013). We found, as reported recently by others, (Egerman et al., 2015) that the Abcam GDF11 antibody readily detected both GDF11 and myostatin (Figure 1A), suggesting that this is not an appropriate reagent to define GDF11 changes with aging or after rGDF11 injection. The Abcam antibody also did not readily detect the non-reduced forms of either GDF11 or myostatin. We then tested the specificity of an R&D systems GDF11 antibody (Figure 1B). This antibody had high specificity for GDF11 versus myostatin and was able to detect both reduced and non-reduced forms of GDF11. This antibody was used to detect GDF11 in the present experiments.

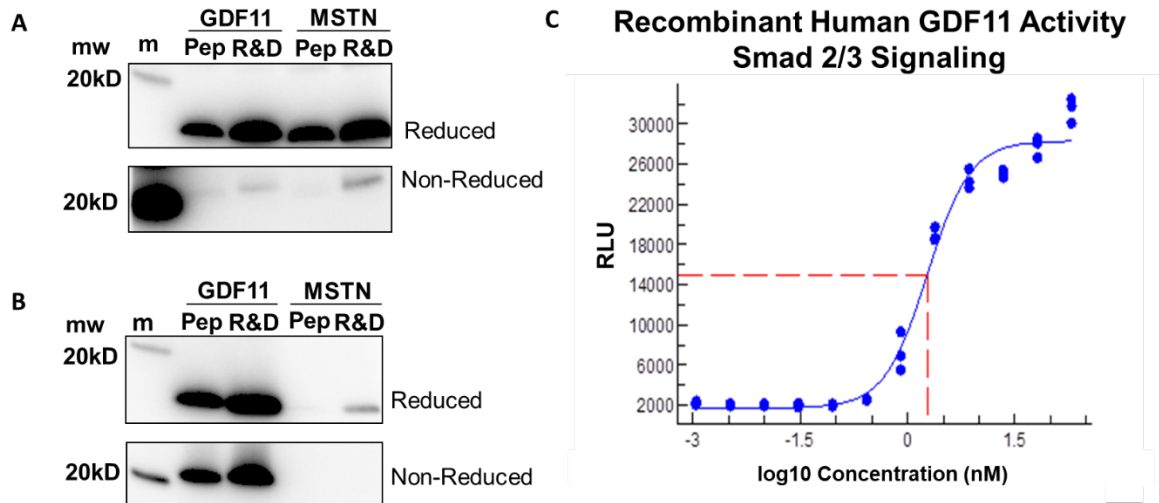


Figure 1. Assessment of antibody reactivity and function of rGDF11. A-B: Western Blot was used to determine the specificity of antibodies against GDF11 and Myostatin (MSTN) (100ng) in reduced vs non-reduced Samples. A: anti-GDF11 Abcam B: anti-GDF11 R&D Systems. The antibody from R&D specifically detected both reduced and non-reduced forms of GDF11. C: Functional activity of rGDF11 (R&D Systems) was determined by ability to activate Smad2/3 signaling in HepG2 reporter cells using a luciferase assay. rGDF11 induced Smad2/3 activity with EC50 and EC90 values of 1.9 nM and 8.6 nM respectively.

We documented the bioactivity of recombinant proteins before injecting them into old mice. The rGDF11 protein was analyzed for its ability to induce Smad2/3 (its known signaling pathway) activity using HepG2 Smad2/3 luciferase reporter cells (Figure 1C). rGDF11 induced Smad2/3 activity with an EC50 and EC90 of 1.9 nM and 8.6 nM respectively (Figure 1C), documenting that rGDF11 binds to its native receptor with high affinity.

GDF11 Blood Levels Increase After Injection of rGDF11

We next performed studies to determine if a daily intraperitoneal injection of rGDF11 (0.1 mg/kg for 28 days) into 24-month-old male mice reverses any existing pathological cardiac hypertrophy. We measured circulating levels of rGDF11 in the plasma of old mice, either 1-3 hours after rGDF11 injection (for peak levels) or 24 hours after injection (for trough levels) (Table 3). These studies showed that rGDF11 rises to a detectable peak within a few hours and then falls to low levels within 24 hours. Importantly, the native GDF11 levels in old mice were below the quantification level (0.1ng/ml) of this assay. Therefore, we were unable to determine if GDF11 levels in the blood decreased with age in C57BL/6 mice, similar to what has been reported recently (Egerman et al., 2015).

GDF11 Has No Effect on Cardiac Hypertrophy

Pathological cardiac hypertrophy was assessed using heart weight to tibia length (HW/TL) and heart weight to body weight (HW/BW) ratios. Heart size was also determined with echocardiographic measures. In addition, immunohistochemistry and qRT-PCR were used to examine cardiac fibrosis and the presence of common markers of PCH. rGDF11-treated 24-month-old male animals were compared to vehicle-treated

Table 3. Circulating levels of GDF11 after injection. Plasma was collected 1.5-2 hours after injection of GDF11 at 0.1mg/kg or vehicle for peak levels (N=11) and 24 hours for trough levels (N=10). BQL=below quantification level (0.1ng/ml).

	Peak	Trough
GDF11	12.8±8.6 (ng/ml)	0.6±0.5 (ng/ml)
Vehicle	BQL	BQL

animals. We also studied 8 or 12 week old young mice to define the magnitude of age dependent pathological cardiac hypertrophy.

Our studies showed that rGDF11 had no effect on the heart weight or body weight of old mice (Figure 2A). Heart weight to body weight (HW/BW) and heart weight to tibia length (HW/TL) ratios were not significantly different between rGDF11 and vehicle treated animals. In addition, the HW/BW ratio of 24-month-old animals was not significantly different from 8 or 12-week-old mice (Figure 2A). These results show that while the heart weight (and body weight) of 24-month-old animals is greater than that of young animals, there is no pathological hypertrophy, but rather normal growth associated with changes in body mass (Freeman et al., 1994; Kiper, Grimes, Van Zant, & Satin, 2013; Savabi & Kirsch, 1992).

Myocyte cross-sectional area was measured in vehicle and rGDF11 treated 24-month-old mouse hearts by performing morphometric analysis of cardiac histological

sections. No differences in myocyte cross-sectional area between rGDF11 and vehicle treated 24-month-old animals were observed (Figure 2B).

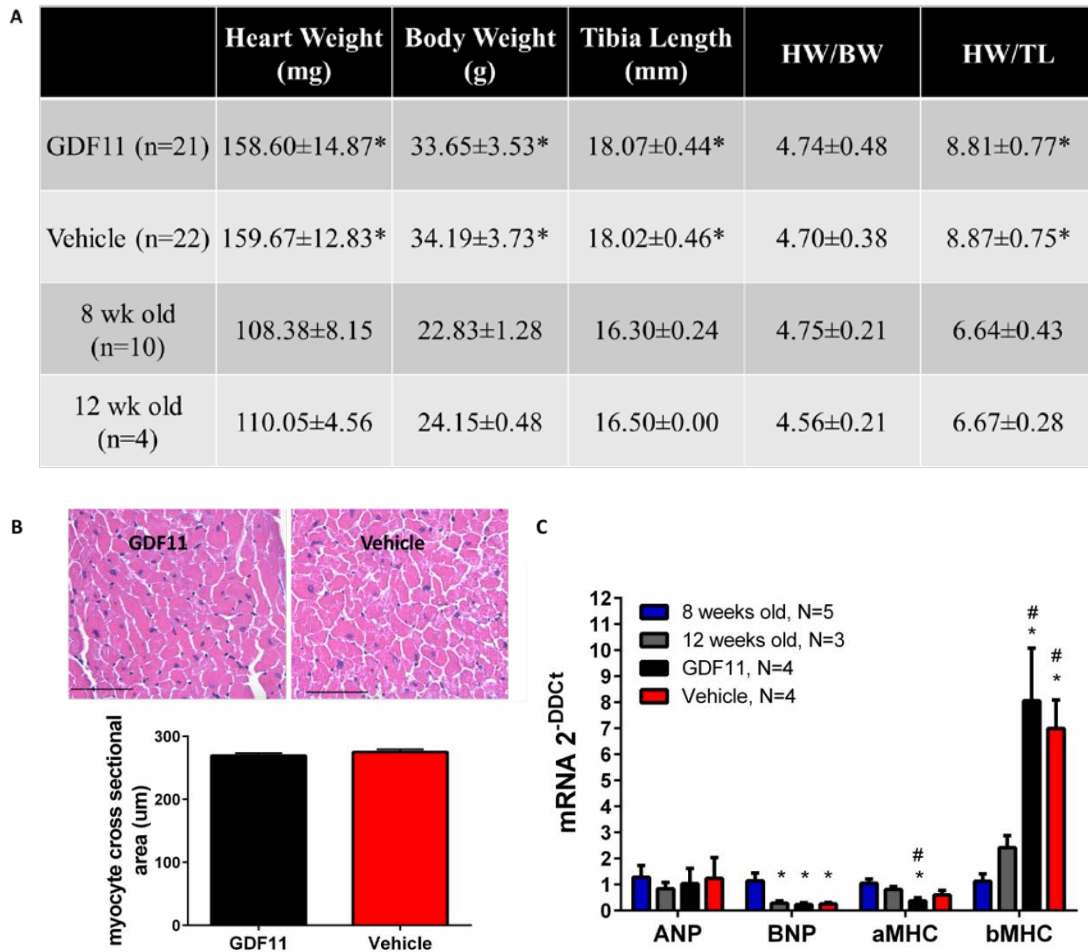


Figure 2. Assessment of hypertrophy in vivo. A: Heart weight, body weight, and tibia length was measured at time of sacrifice 28 days post initial injection of GDF11. No significant differences were found between GDF11 and vehicle treated animals. $*=p \leq 0.05$ compared to 8-week-old mice. B: There was no difference in myocyte cross sectional area between rGDF11 and vehicle treated animals. 100-175 myocytes with nuclei from 6 animals were analyzed per group Scale bar= 50 microns. C: There was no difference in ANP levels between young and aged mice. There was no significant difference between

GDF11 and vehicle treated animals. * $p < 0.05$ vs 8-week-old mice. # $p < 0.05$ vs 12-week-old mice.

mRNA levels of the hypertrophic markers ANP, BNP, α MHC, and β MHC were also measured in vehicle and rGDF11 treated 24-month-old mice. We also compared young and old mice to explore age related changes in these parameters. There were no significant differences in ANP, BNP, α MHC, or β MHC mRNA expression between rGDF11 and vehicle treated animals (Figure 2C). While there were no differences in ANP mRNA levels between young and aged mice, BNP was greater in 8-week-old animals versus other ages. In addition, there appear to be age related reductions in α MHC mRNA and increases in β MHC. These likely represent maturational changes in these molecules (Pandya, Kim, & Smithies, 2006).

Cardiac fibrosis was measured in vehicle and rGDF11 treated 24-month-old mice by measuring the percentage of collagen in cardiac histological sections using Masson's trichrome staining. There was no significant difference in fibrosis between rGDF11 and vehicle treated animals (Figure 3A). We also tested the ability of rGDF11 to stimulate fibroblast activation in-vitro using primary cultures of normal human dermal fibroblasts. rGDF11 stimulated fibroblast activation with an EC50 of 176pM (Figure 3B). This was similar to the effects of myostatin, which had an EC50 of 83pM.

GDF11 Had No Effect on Cardiac Function

Cardiac structure and function remained unchanged at 1, 2, and 4 weeks of rGDF11 treatment as measured by echocardiography (Figure 4A-B.) In terminal hemodynamic studies, there was no difference in max pressure, max dP/dT, min dP/dt, EDP, or Tau

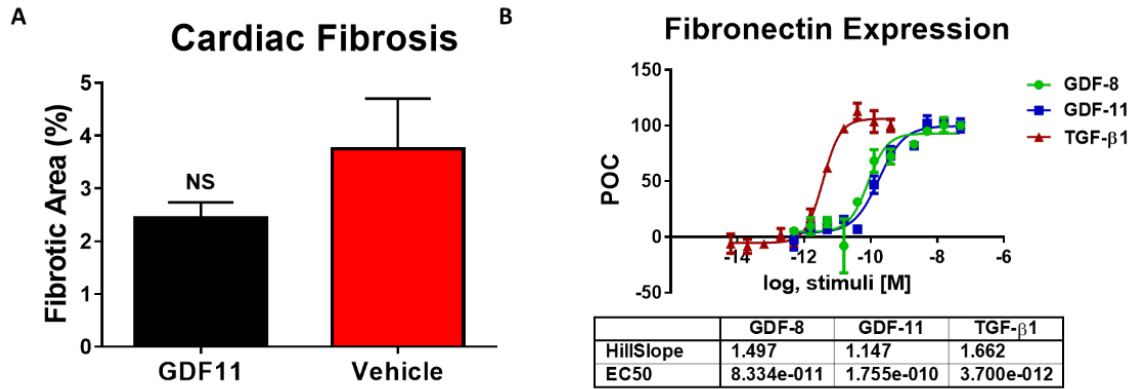


Figure 3. Analysis of cardiac fibrosis. A: Percent fibrosis was determined in histological sections using Masson's trichrome staining by measuring the percentage of collagen (stained in blue) out of the total myocardial area. There was no significant difference in fibrotic area between rGDF11 (n=6) and vehicle treated animals (n=6). NS= Non-Significant B: The effect of rGDF11 on fibroblast activation in vitro was examined by measuring fibronectin expression using normal human dermal fibroblast treated with a titration of TGF-β1, GDF-11, or GDF-8 at 1:3 dilutions, or medium. Fluorescence intensity values are plotted as a percent change from medium control (POC). GDF11 stimulated fibronectin expression with an EC50 of 176pM.

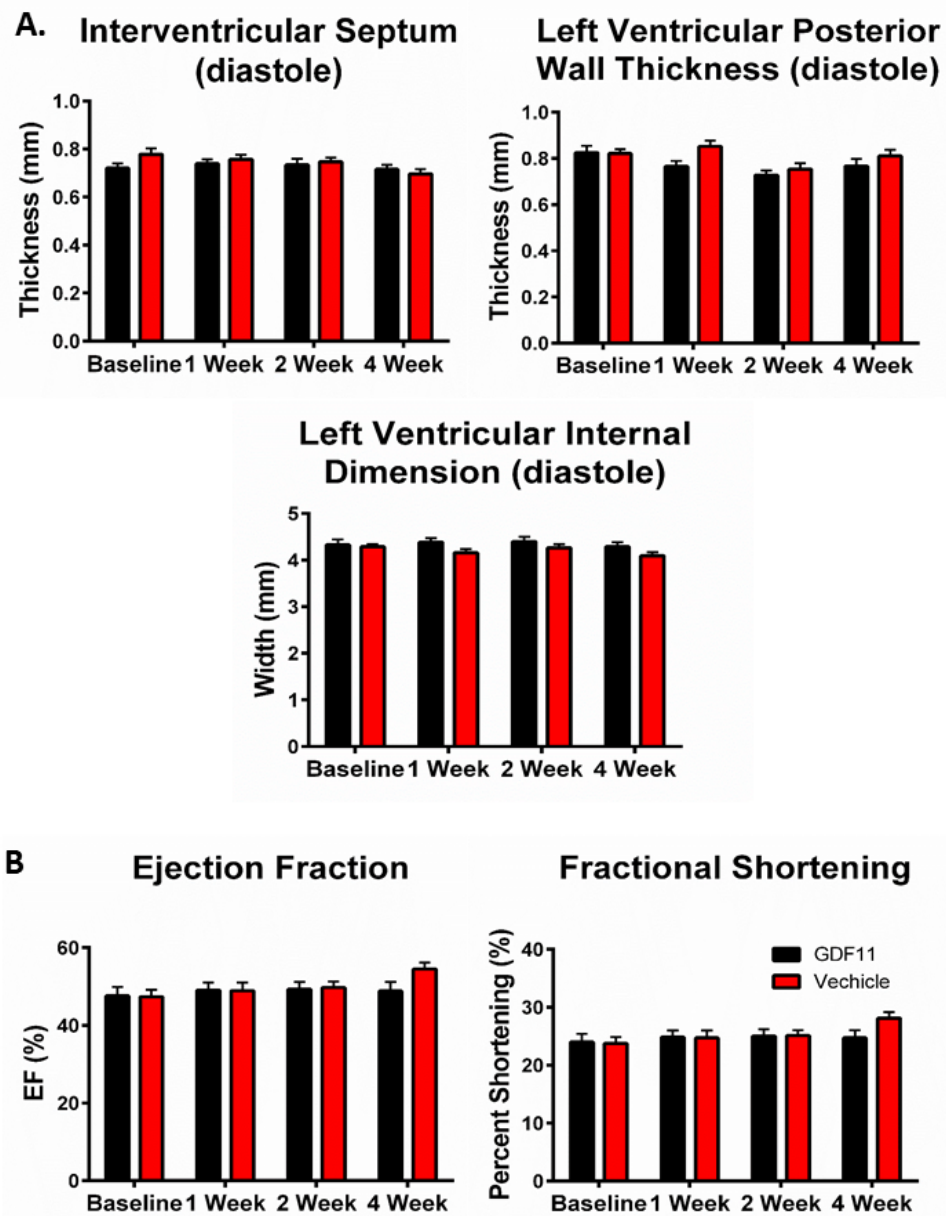


Figure 4. Cardiac structure and function measured by echocardiography. Mice received echocardiography at baseline, 1, 2, and 4 weeks after the start of injections. rGDF11 did not affect any A: structural or B: functional parameters measured. rGDF11 (n=21) or vehicle (n=22)

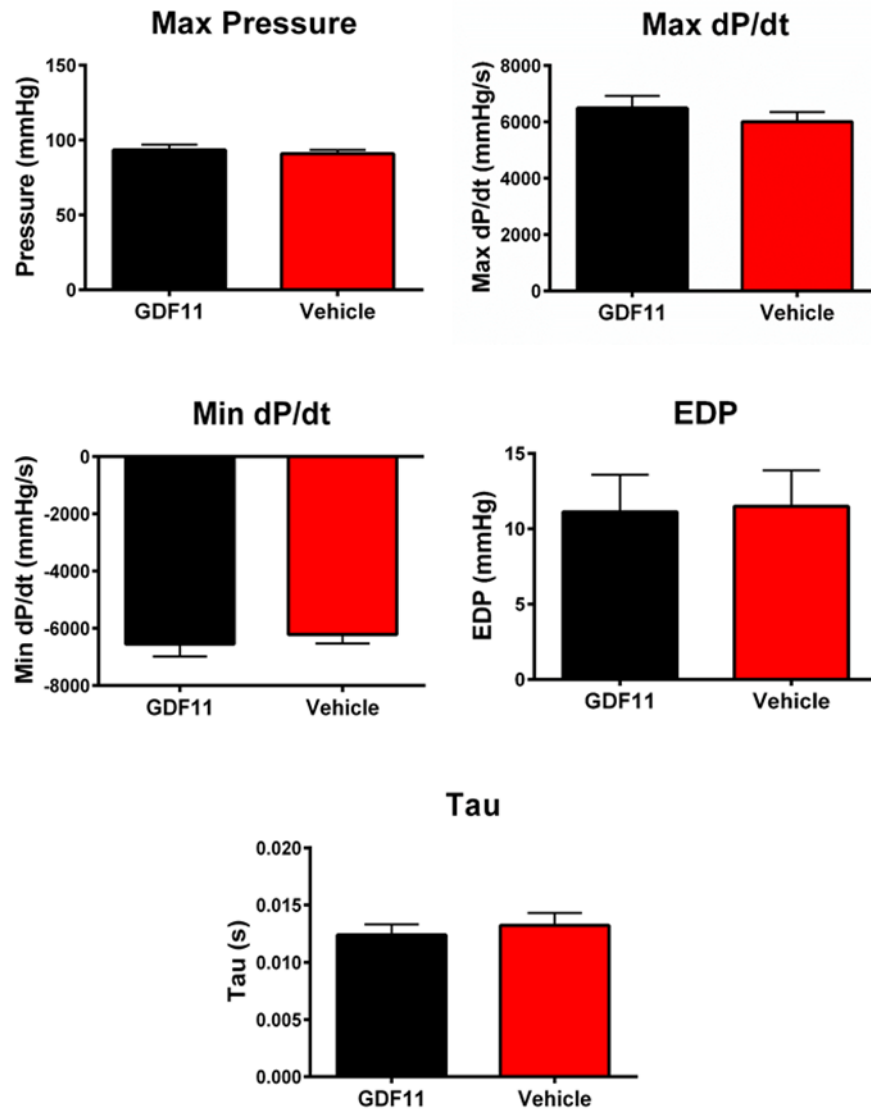


Figure 5. Intra-left ventricular pressures. In vivo intra-LV pressures were measured at time of sacrifice. There was no difference in max pressure, max dP/dT, min dP/dt, EDP, or Tau between rGDF11 (n=21) and vehicle (n=22) treated animals.

between rGDF11 and vehicle treated animals (Figure 5). Collectively these experiments show that rGDF11 had no effects on cardiac structure or function.

GDF11 Did Not Prevent Phenylephrine-Induced Hypertrophy In Vitro

Finally, we tested the effects of rGDF11 treatment on phenylephrine-induced hypertrophy in cultured neonatal rat ventricular myocytes (NRVMs)(Loffredo et al., 2013). NRVMs were treated with rGDF11 at three concentrations: 0.5nM, 5nM, and 50nM with and without simultaneous phenylephrine treatment. rGDF11 treatment failed to inhibit phenylephrine-induced increases in myocyte surface area, but instead caused a dose dependent increase in myocyte size (Figure 6A). rGDF11 failed to inhibit phenylephrine-induced increases in ANP and BNP mRNA expression, while by itself it induced a dose-related increase in ANP and BNP mRNA compared to controls (Figure 6B-C).

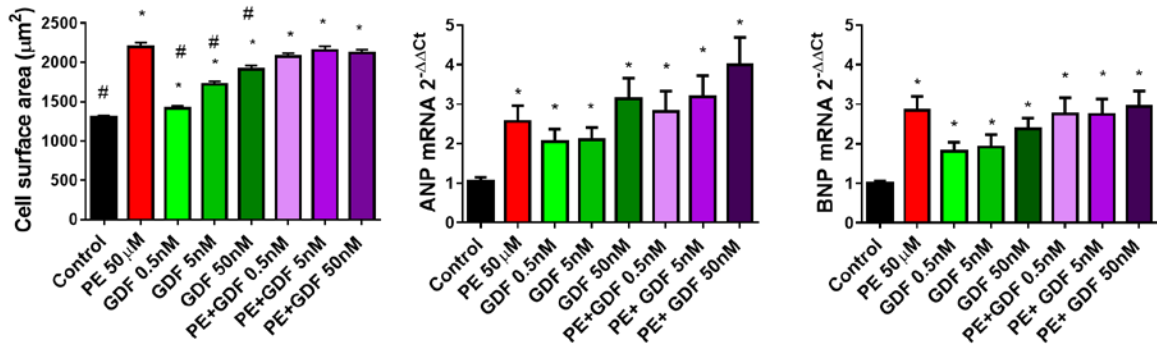


Figure 6. GDF11 induces hypertrophy in NRVMs. A: 150-300 myocytes were analyzed from at least 20 fields of view per condition B-C: GDF11 treatment increased expression of ANP and BNP mRNA expression (n=3) * $p < 0.05$ vs control. # $p < 0.05$ vs PE 50µM.

Discussion

Aging related cardiomyopathy is often secondary to the accumulation of cardiovascular disease (CVD) and disease-induced changes in cardiac structure and function lead to cardiomyopathy (Barouch et al., 2003; Bujak et al., 2008; Waller, 1988). True age dependent changes in cardiac structure and function in CVD-free individuals are not well understood and if defined could provide novel clues for protection from aging-specific cardiac functional decline.

Others have searched for aging-specific changes in factors that circulate in the blood that if corrected could prevent or reverse age dependent decline in the function of critical organ systems (Conboy et al., 2005; Ruckh et al., 2012). Indeed, a recent study, which has generated a significant amount of attention and collateral reporting (<http://hsci.harvard.edu/aging-and-gdf11-what-we-know>), (<http://www.nature.com/cr/journal/v24/n12/full/cr2014107a.html>), suggests that the blood levels of the myostatin-related protein, growth differentiation factor 11 (GDF11), decreases with age (Loffredo et al., 2013). These myokine proteins are members of the transforming growth factor β (TGF β) family of proteins. Myostatin can potently inhibit skeletal muscle growth and differentiation (McPherron, Lawler, & Lee, 1997), with smaller effects on cardiac muscle (Cohn, Liang, Shetty, Abraham, & Wagner, 2007). Reductions or loss of function of myostatin causes increases in skeletal muscle mass, with little or no effect on the heart (Heineke et al., 2010; Mosher et al., 2007; Parsons et al., 2006).

A recent study reported that the circulating level of GDF11 decreases with aging, and this reduction correlated with the development of pathological cardiac hypertrophy in old mice (Loffredo et al., 2013). Pathological cardiac hypertrophy was rescued in these old

mice by either restoring a “youthful” circulation with parabiosis or by injection of rGDF11 to restore youthful GDF11 levels (Loffredo et al., 2013). Related studies suggest that restoring youthful GDF11 levels rejuvenates skeletal muscle (Sinha et al., 2014) and brain (Katsimparidi et al., 2014) structure and function. These findings suggest that restoring youthful levels of GDF11 can reverse aging dependent decline of critical organ systems and they were highly touted as the discovery of the long sought after tissue rejuvenation factor (<http://hsci.harvard.edu/aging-and-gdf11-what-we-know>). However, the skeletal muscle findings have recently been challenged (Egerman et al., 2015) and, considering our results in the old heart, it does not appear that GDF11 is an anti-aging factor (<http://stemcellassays.com/2015/05/gdf11-controversy-antibody-better/>) (http://pipeline.corante.com/archives/2015/05/20/a_young_blood_controversy.php) (<http://www.nature.com/news/young-blood-anti-ageing-mechanism-called-into-question-1.17583>). A recent editorial has also highlighted that GDF-11 is not the long sought rejuvenation factor (Brun & Rudnicki, 2015).

The objectives of our experiments were to reexamine the idea that rGDF11 is a critical cardiac anti-aging factor in the mouse (Loffredo et al., 2013). Our goal was to define the mechanisms underlying the ability of rGDF11 to reverse aging dependent cardiac pathological structural and functional remodeling.

We first set out to develop assays with appropriate sensitivity and specificity for GDF11 detection. We first examined the antibody used in previous work (Loffredo et al., 2013) and found, similar to results in another recent report (Egerman et al., 2015), that this antibody also identified the highly homologous family member, myostatin (Online figure IA). We then characterized an antibody (R&D systems) that detected GDF11 and not

myostatin (Figure 1B) and we used this antibody to determine that treatment increases blood levels of rGDF11 in old mice. We found that endogenous levels of GDF11 were below our detection limits in both young and old mice. Therefore, we could not determine if GDF11 levels fell with age similarly to what has been reported recently in a study of skeletal muscle (Egerman et al., 2015). Our results show that the reagents used in previous work (Loffredo et al., 2013) are inadequate to determine if GDF11 levels fall in old mice or increase after rGDF11 treatment.

Our studies show that treatment of old mice with rGDF11 had no effect on heart or myocyte size, overall cardiac structure and cardiac pump function (Figures 2, 4, 5). Indeed, hearts and their myocytes are larger in old versus young mice (Helms et al., 2010; X. Zhang, Azhar, Furr, Zhong, & Wei, 2003). However, old mice have greater body weights than young mice and 24-month-old mice have the same HW/BW ratio as 8 or 12-week-old mice, which is inconsistent with the presence of pathological hypertrophy. In addition, we could not find evidence for activation of pathological hypertrophy signaling in old animals. Collectively our results suggest that the increase in heart size with aging is what is expected in healthy animals that have increases in their body mass. There are numerous reports showing that heart size changes with increases or decreases in body size in mature adult animals (Ernsberger, Koletsky, Baskin, & Collins, 1996; Lim et al., 2000). Our results suggest that HW/TL cannot discriminate between pathological hypertrophy and physiological growth in mature animals where tibia length does not change.

The suggestion of an anti-hypertrophic effect of a youthful circulation in old mice came from parabiosis experiments in which old and young mice had a shared circulation (Loffredo et al., 2013). In these studies, heart size was clearly reduced in old mice sharing

a circulation with young mice (Loffredo et al., 2013). However, the old mice lost 25-30% of their body weight during the month of parabiosis with the young mice and the HW/BW ratios in these old mice appear to have been unchanged. The unexplained data in this previous report (Loffredo et al., 2013), upon which the conclusions in the parabiosis experiments rest, is that there was no change in the HW of old mice sharing a circulation with other old mice, even though these old mice also lost 25% of their body weight. The observation that mice can reduce their BW by 25% with no corresponding change in HW (Loffredo et al., 2013) does not fit with a large body of existing work (Ernsberger et al., 1996; Lim et al., 2000; Savabi & Kirsch, 1992).

We also studied the effects of GDF11 on phenylephrine-induced hypertrophy of neonatal rat ventricular myocytes. We found that rGDF11, by itself, activated pathological hypertrophy signaling and increased myocyte size, but it did not exacerbate or block the effects of phenylephrine reported previously (Loffredo et al., 2013).

In summary, our studies show that daily injections of biologically active rGDF11 raised the blood levels of rGDF11 in old mice but had no effect on heart and myocyte size; overall cardiac structure and cardiac pump function. We also did not find evidence for the existence of pathological hypertrophy in 24-month-old disease-free C57BL/6 mice. These results do not support the idea that GDF11 should be part of an “anti-aging” elixir.

CHAPTER 3

GDF11 IN PRESSURE OVERLOAD INDUCED CARDIAC HYPERTROPHY

Abstract

Rationale

There have been conflicting reports on the effects of Growth Differentiation Factor 11 (GDF11) on the normal, diseased, and aging heart. GDF11 has been reported to reverse aging induced hypertrophy, but this observation has not been well validated. Excess GDF11 has also been shown to cause cardiac and skeletal muscle wasting. These controversies could be resolved if dose dependent GDF11 effects were documented in normal and aged animals as well as in pressure overload induced pathological hypertrophy.

Objective

To determine dose dependent effects of GDF11 on normal hearts and those with pressure overload induced cardiac hypertrophy.

Methods and Results

12-13-week-old C57BL/6 mice underwent transverse aortic constriction (TAC) surgery. One-week post TAC, these mice received a daily intraperitoneal injection of either vehicle or recombinant GDF11 at one of 3 doses: 0.5 mg/kg, 1.0 mg/kg, or 5.0 mg/kg for 14 days. Treatment with GDF11 increased plasma concentrations of GDF11 and p-SMAD2. There were no significant differences in the peak pressure gradients across the aortic constriction between treatment groups at one-week post-TAC. Two weeks of GDF11 treatment caused dose dependent decreases in cardiac hypertrophy as measured by HW/TL ratio, myocyte cross sectional area, and LV mass. Pathological cardiac hypertrophy markers including BNP, alpha skeletal actin, beta myosin heavy chain, and alpha myosin

heavy chain were changed with GDF11 treatment. GDF11 improved cardiac pump function while preventing TAC-induced ventricular dilation and caused a dose dependent decrease in interstitial fibrosis. However, treatment with the highest dose (5.0mg/kg) of GDF11 caused severe body weight loss, with significant decreases in both muscle and organ weights in both sham and TAC mice.

Conclusions

GDF11 can reduce pathological cardiac hypertrophy and associated fibrosis in pressure overload. However, the therapeutic range for these beneficial GDF11 effects appears quite narrow with slightly higher GDF11 doses causing cachexia and death.

Introduction

Cardiovascular diseases result in over 600,000 deaths in the United States alone, with high blood pressure as a primary or contributing cause to more than 400,000 deaths annually (Benjamin et al., 2017; Kearney et al., 2005). Prolonged high blood pressure initially results in concentric pathological hypertrophy, which if left untreated can lead to heart failure with (Heart Failure with reduced Ejection Fraction; HFrEF) or without (Heart Failure with preserved Ejection Fraction; HFpEF) ventricular dilation and depressed cardiac ejection fraction. Both of these clinical situations also exhibit altered left ventricular (LV) diastolic function that is associated with interstitial fibrosis, decreased LV systolic reserve, increased arterial stiffness, and impaired endothelial function (Lakatta & Levy, 2003a, 2003b). With sustained disease stress these structural and functional changes are accompanied by increased cardiomyocyte death from apoptosis and/or necrosis. Since the heart has little regenerative capacity (Rumyantsev, 1977; Soonpaa & Field, 1997), myocyte death leads to decreased numbers of functional cardiac myocytes (Goldspink,

Burniston, & Tan, 2003; Olivetti, Melissari, Capasso, & Anversa, 1991). Current therapies for hypertension (HPT) and heart failure are somewhat effective, but do not reverse many of the disease induced cardiac alterations. There is a need to identify new therapeutic targets that could slow or reverse adverse cardiac remodeling in acquired cardiovascular diseases such as HPT, and especially in HFpEF, where there are inadequate therapeutic options.

Members of the TGF- β super family of proteins are involved in a wide range of diverse functions and play critical roles in embryogenesis, development and overall tissue homeostasis. This family of proteins is known to be involved in tissue growth and repair but can be dysregulated in cardiovascular disease. Members of this family have diverse roles in the regulation of differentiation, apoptosis, cell migration, adhesion, and extracellular matrix deposition (Vilar, Jansen, & Sander, 2006) and are being examined as possible therapeutic targets in cardiovascular disease (Angelov et al., 2017; Biesemann et al., 2015; Biesemann et al., 2014).

Growth Differentiation Factor 11 (GDF11) is a member of the TGF- β super family of proteins and is highly homologous to the well-studied TGF- β family member, myostatin. Myostatin is a known negative regulator of skeletal muscle growth (Mosher et al., 2007; Parsons et al., 2006). Given its structural similarity to myostatin, GDF11 has been suggested to have a similar effect on skeletal and cardiac muscle (Xing et al., 2007). Supporting this idea are recent studies in which circulating GDF11 levels have been increased and result in skeletal and cardiac muscle wasting (Hammers et al., 2017; Zimmers et al., 2017). These studies documented that overexpression of GDF11 from AAV-2 or CHO cells resulted in decreases in cardiac and skeletal muscle mass and function

and could even induce death of mice at high doses. Interestingly, other studies have shown that GDF11 has little or no effects on cardiac or skeletal muscle mass (Smith et al., 2015), and there is some data suggesting that GDF11 treatment can have beneficial effects on the heart (Du et al., 2017; Poggioli et al., 2016).

Previous studies on the effects of GDF11 on the normal and diseased heart have produced widely variant findings and conclusions. One series of studies suggested that circulating GDF11 levels decrease with age and are associated with pathological cardiac hypertrophy. When normal levels were restored with daily injections of recombinant protein, they rejuvenated the aged heart (Loffredo et al., 2013), skeletal muscle (Sinha et al., 2014), and brain (Katsimpardi et al., 2014). These studies suggest that daily injections of GDF11 reverse aging induced pathological hypertrophy (Loffredo et al., 2013), improved skeletal muscle function (Sinha et al., 2014), and improved brain vascularization (Katsimpardi et al., 2014). However, a number of more recent studies could not validate these results (Egerman et al., 2015; Smith et al., 2015). Our group has shown that the (0.1 mg/kg/day) dose of GDF11 reported to reverse aging induced cardiac pathologies (Loffredo et al., 2013) had no effect on cardiac function or structure in aged C57BL/6 mice (Smith et al., 2015). No age-related pathological cardiac hypertrophy was observed in these studies (Smith et al., 2015).

A major purpose of the present study was to bring some clarity to the disparate findings reported regarding GDF11 effects on the heart and skeletal muscle in adult mice. In our view, performing studies with recombinant proteins in different laboratories and achieving identical results is clearly challenging, in part because differences in dosing or in the biological activity of the recombinant protein are not easily controlled. These

problems might explain some of the disparate results in the literature. Therefore, to clarify some of the discrepancies in this field, we performed a (blinded) dose ranging study in which we treated 12-13-week-old C57BL6 mice with GDF11 for 14 days, beginning one week after undergoing transverse aortic constriction (TAC) or sham surgery. This allowed us to explore dose dependent GDF11 effects on the structure and function of normal hearts (and skeletal muscle) as well as those with evolving pathological cardiac hypertrophy. Our results show that daily injections of GDF11 caused a dose dependent reduction in body weight and heart mass in both normal and TAC mice, with a disproportionate effect on heart weight in TAC mice. Our results are consistent with the hypothesis that GDF11 can reduce pathological hypertrophy and associated fibrosis in pressure overload. However, the therapeutic range for these beneficial GDF11 effects appears quite narrow with slightly higher GDF11 doses causing cachexia and death.

Methods

Animals

C57BL/6 male mice aged 12 weeks were purchased from the Jackson Laboratories. All animal studies were performed according to protocols approved by the Institutional Animal Care and Use Committee of Lewis Katz School of Medicine at Temple University and conducted in accordance with the *Guide for the Use and Care of Laboratory Animals*.

Animal Model of Cardiac Hypertrophy

Mice received either sham surgery (55 mice) or transverse aortic constriction surgery (120 mice). Mice were anesthetized via inhalation of 2.5% isoflurane and artificially ventilated. The transverse aortic arch was accessed via partial thoracotomy to the second rib and the aortic arch was constricted between the innominate artery and left

carotid arteries using a 7-0 silk suture tied firmly against a 27-gauge blunted needle. The needle was promptly removed, the chest was closed, and the mice were allowed to recover from anesthesia. The sham-operated mice underwent the same operation except for aortic constriction. Ligation of the aorta was confirmed one week after TAC using pulse wave doppler echocardiography (ECHO). Mice with a maximum peak gradient of less than 30 were excluded from the study.

GDF11 Dosing and Injections

Investigators were blinded to treatment. Mice were given a daily single intraperitoneal injection of either rGDF11 (R&D Systems) at 0.5mg/kg (N=40, 15 sham, 20 TAC), 1.0 mg/kg (40, 15 sham, 20 TAC) or 5.0 mg/kg (N=25, 10 sham, 15 TAC) or vehicle (60mM NaAcetate Buffer, pH 5.0 and 10% Trehelose) (N=40, 15 sham, 20 TAC) for 14 days beginning one week after TAC surgery. rGDF11 stock solution was dissolved in NaAcetate Buffer, pH 4.5 at a concentration of 1mg/ml. Stock solutions were diluted with the dosing solution (60mM NaAcetate Buffer, pH 5.0 and 10% Trehelose) to reach the final concentrations of 0.5mg/kg, 1.0 mg/kg or 5.0 mg/kg. Boehringer Ingelheim Pharmaceuticals provided all solutions in a blinded fashion. Mice were assigned to treatment groups so that there were no significant differences in ejection fraction, wall thicknesses, left ventricular mass, or pressure gradients at the band between the groups at one week. Mice were weighed every day before dosing.

Echocardiography

Mice were anesthetized with 2-2.5% isoflurane and then maintained at 1.5-2%. Anesthetized mice underwent transthoracic echocardiography using a Vevo2100 ultrasound system (VisualSonics; Toronto, Canada). Repeated measurements were

performed at baseline and at 1, and 3 weeks post-surgery. Hearts were viewed in the short-axis at the level of the mid-papillary muscles for M-mode. Parameters were to be measured offline (Vevo software) including end diastolic diameter (EDD), end-systolic diameter (ESD), left ventricular posterior wall thickness (LVPW), and left ventricular anterior wall thickness (LVAW) to determine cardiac morphological changes. Ejection fraction (EF) and fractional shortening (FS). Images were acquired in the short-axis B-mode and M-mode for analysis of cardiac function and dimensions. Pulse wave doppler of the transverse aorta was used to measure the peak pressure gradients at the aortic constriction.

Circulating Levels of GDF11

An MSD assay to detect human recombinant GDF11 was developed using a homogenous assay format. A master mix was prepared, combining 4.0 µg/mL biotinylated anti-GDF11 antibody (R&D Systems) and 2.0 µg/mL sulfo-labeled anti-GDF11 antibody (R&D Systems) in binding buffer (5% BSA in 1X PBS with 0.05% Tween 20). This master mix was added to a 96-well, non-binding, light-blocking plate (Fisher Scientific) at 50 µL per well. Twenty-five µL of standards, QCs, and mouse plasma samples (diluted 2-fold in binding buffer) were added per well in duplicate to the non-binding plate containing the master mix. The non-binding plate was incubated at room temperature on a plate shaker (600 rpm, 2 hours). In parallel, an MSD streptavidin (SA) gold 96-well plate (Meso Scale Discovery) was blocked using 150 µL blocking buffer (5% BSA with 1X PBS with 0.05% Tween 20) and incubated at room temperature on a plate shaker (500 rpm, 2 hours). After incubation, the MSD plate was washed three times with 300 µL per well wash buffer (0.05% Tween 20 in 1X PBS). Fifty microliter aliquots of each sample mix from non-binding plates were added to MSD plates and incubated at room temperature on a plate

shaker (600 rpm, 2 hours). After incubation, the plate was washed three times and 150 μ L of 2x Read Buffer T (MSD, stock diluted 2X in H₂O) was added to each well and read immediately on the MSD QuickPlex 120 instrument using an electrochemiluminescent (ECL) signal. Quality control and unknown mouse plasma sample concentrations were back-calculated using standard curves fitted to a four-parameter logistics equation using MSD Discovery Workbench software.

Histology, Weight Measurements, Myocardial Fibrosis and Myocyte Cross Sectional Area

Prior to sacrifice rGDF11 and vehicle treated animals were randomly divided to be used for molecular analysis or histology. The mice receiving the 5 mg/kg dose of GDF11 had to be euthanized after 9 to 10 doses of GDF11 due to severe cachexia. All other mice were euthanized after 14 days of treatment with GDF11 or Vehicle. All Tissues were rinsed with PBS, excess fluid was blotted off, and weighed. Tibias were removed and measured to the nearest 0.5 mm. The hearts from approximately two-thirds of the mice per group were immediately snap-frozen in liquid nitrogen for molecular analysis. The remaining hearts were perfusion-fixed with 10% formalin and paraffin embedded for histology following previously published protocols (see supplemental material references 3-5). Tissue blocks were sent to AML Laboratories (St Augustine, FL) for sectioning and staining for Hemotoxylin and Eosin. Myocyte cross sectional area was measured from 3-8 mice per group using slides stained with Wheat-Germ agglutinin. 3-8 samples from each group were stained with Masson's trichrome (Sigma-Aldrich; St. Louis, MO) for collagen deposition. Myocyte cross-sectional area and Fibrotic area were quantitated with NIH ImageJ software (<http://rsbweb.nih.gov/ij/>). At least 300 myocytes from 3 sections of the

heart were analyzed per animal to assess myocyte cross sectional area. At least 13 fields of view were analyzed per animal for collagen deposition. Fibrotic area was measured by visualizing all blue-stained areas. Color based- thresholding was used to differentiate between the total area of collagen deposition, stained in blue, and myocyte areas stained red in each section. Fibrosis is presented as the sum of the blue-stained areas divided by total ventricular area. Interstitial fibrosis was measured from images that did not include vessels, while perivascular fibrosis was measured from areas with both myocytes and vessels.

Western-Blot Analysis

Snap-frozen hearts were cut in half. One half of the heart was used for RNA isolation and the other half for protein isolation. Frozen heart sections were homogenized in RIPA buffer (Sigma) with phosphatase inhibitor cocktails 1 and 2, a protease inhibitor cocktail and EDTA added at a 1x concentration. Protein was quantified using the Pierce BCA Protein Assay Kit (Thermo Scientific). Tissue homogenates were resolved on 4-15% gels (Biorad) under reducing conditions and transferred to nitrocellulose membranes. Membranes were blocked for 1 hour in Odyssey Blocking Buffer (LI-COR). The following primary antibodies were used for immunoblotting: pSMAD2, SMAD2 at 1:1000 (CellSignaling Technology, Danvers, MA, USA). LI-COR goat anti-rabbit or goat anti-mouse secondaries were used at 1:5000 concentration. Odyssey CLx western blot detection system (LI-COR, Lincoln, NE, USA) was used to detect the signal.

Real-Time Polymerase Chain Reaction (PCR)

Total RNA was extracted from snap frozen myocardial tissue utilizing TRIzol Reagent (Thermo Fisher) and digested with DNase I (Invitrogen) to eliminate genomic

DNA. cDNA was synthesized using the SuperScript III first strand synthesis system for RT-PCR (Invitrogen) according to the manufacturer's instructions. Real-time PCR was performed using the Quantifast Sybrgreen PCR kit (Qiagen) and The StepOnePlus Real-Time PCR system (Applied Biosystems). Ct values were normalized with respect to beta-2 microglobulin (β 2M). Fold change was calculated with respect to sham vehicle. The primer sets are listed in table 4.

Table 4. Primer sequences for RT-PCR.

Gene	Sequence
β 2M F	5'-ATGTGAGGCGGGTGGAACTG-3'
β 2M R	5'-CTCGGTGACCCTGGTCTTTCTG-3'
<i>Act1</i> F	5'-TGAAGCCTCACTTCCTACCCT-3'
<i>Act1</i> R	5'-CCGTTGTCACACACAAGAGC-3'
α MHC F	5'-ATAAAGGGGCTGGAGCACTG-3'
α MHC R	5'-GTAGCGCTCCTTGAGGTTGT-3'
β MHC F	5'-TCCTGCTGTTTCCTTACTTGCT-3'
β MHC R	5'-GAACTTGGGTGGGTTCTGCT-3'
<i>BNP</i> F	5'-CTGCTGGAGCTGATAAGAGA-3'
<i>BNP</i> R	5'-AGTCAGAACTGGAGTCTCC-3'

Statistics

Data are represented as mean \pm SEM. For echocardiography parameters with repeated measures, linear mixed-effects models were used to determine predicted mean values at each assessment point (baseline, week 1, and week 3) and to test treatment group differences. In each linear mixed-effects model, time and treatment group were included as fixed effects with time-by-treatment group interaction term. T-tests were used to determine significance between sham and TAC mice with vehicle treatment for parameters with a single measurement. One-way analysis of variance evaluated the differences for parameters measured at a single time point within the sham or TAC group using Dunnett's multiple comparison test. Statistical analyses were performed using SAS 9.4 (SAS Institute, Cary, NC) and GraphPad prism version 7.0. A p-value of < 0.05 was used to determine significance for all statistical tests.

Results

GDF11 Causes Dose Dependent Activation of SMAD2 Signaling

The canonical signaling pathway for GDF11 involves activation (phosphorylation) of SMAD2/3. Our results show that rGDF11 injections caused a dose dependent increase in the circulating plasma concentrations of GDF11 (measured 1-1.5 hours after injection on the day of sacrifice) in both sham and TAC mice (Figure 7A). These studies also showed that TAC induced phosphorylation of SMAD2 and treatment with GDF11 increased SMAD2 phosphorylation in both sham and TAC mice (Figure 7B,C). These results support the idea that GDF11 causes a dose dependent activation of SMAD signaling in the normal and hypertrophied heart.

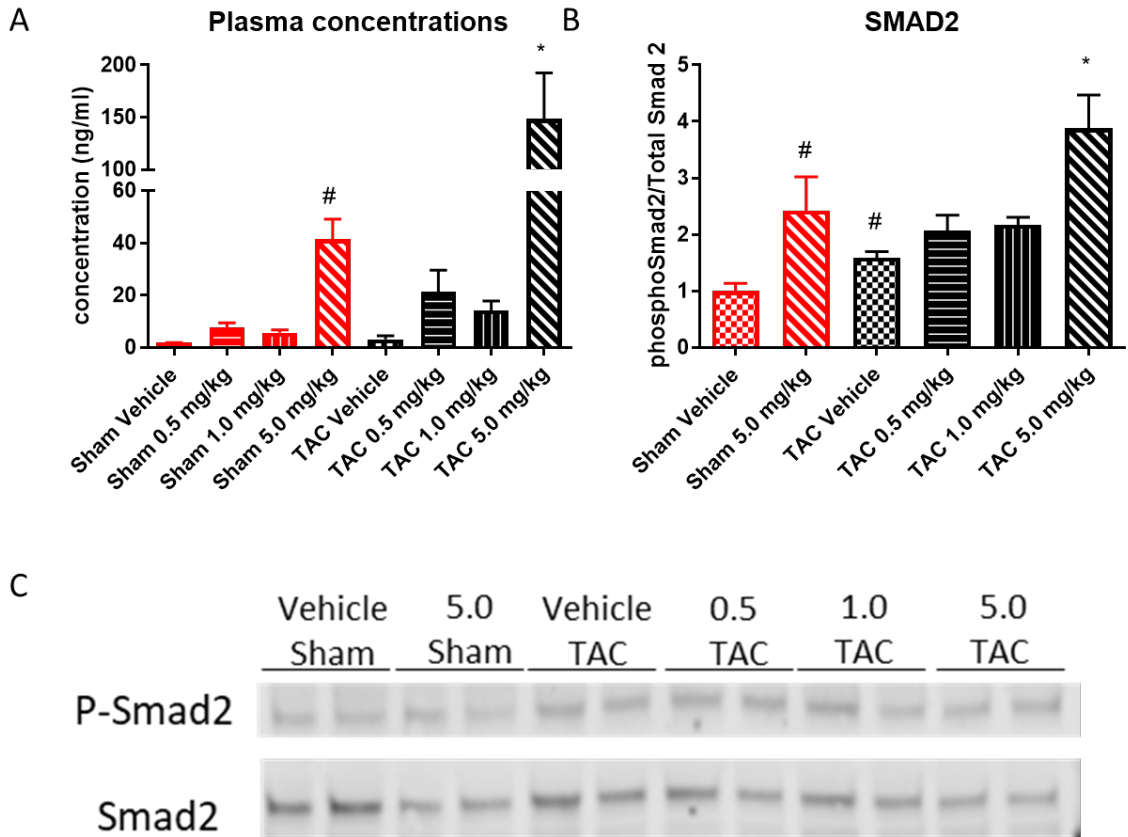


Figure 7. Injections of rGDF11 increase the circulating concentration of GDF11 and SMAD2 phosphorylation. A: Plasma was collected 1-1.5 hours after injection of GDF11 or vehicle. Blood GDF11 levels increased with GDF11 dose. B: Ratio of phosphorylated to total forms of SMAD2 protein in the hearts of vehicle-treated and GDF11-treated TAC and sham mice was quantified by densitometry. (n=5-8 per group) C: Immunoblotting for phosphorylated and total forms of SMAD2 in the hearts of vehicle-treated and GDF11-treated TAC and sham mice. * $p < 0.05$ vs vehicle-treated TAC mice. # $p < 0.05$ vs vehicle-treated sham mice.

GDF11 Decreases TAC-Induced Cardiac Hypertrophy

Pulse wave doppler-based echocardiography (ECHO) techniques were used one week after sham or TAC surgery to determine the peak pressure gradient across the aortic constriction. TAC caused a significant increase in the peak pressure gradient across the constriction in TAC mice (Figure 8A). TAC mice were then randomized to either GDF11 or vehicle treatment groups so that there were no significant differences in the peak pressure gradients at the time of initial treatment (Figure 8A). 3 weeks of TAC (without GDF11 treatment) caused significant increases in heart weight (HW; Table 5), HW/body weight (BW) (Figure 8B), HW/tibial length (TL) (Figure 8C) and left ventricular myocyte cross sectional area (CSA) (Figure 9A,B) versus vehicle treated sham mice. ECHO-based evaluation of LV anterior wall thickness and cardiac mass also documented a significantly greater pathological hypertrophy in vehicle-treated TAC mice versus sham (Figures 10A,D). Traditional markers of pathological LV hypertrophy were also significantly changed in vehicle-treated TAC versus sham mice (Figure 9C-F). These results show that the TAC performed in these studies induced well documented features of pathological hypertrophy in vehicle-treated mice.

Daily intraperitoneal injections of GDF11 were started one week after TAC or sham surgery and continued for up to two weeks at doses of 0.5/1/or 5 mg/Kg (Figure 11A,B). In sham mice, GDF11 doses of 0.5 and 1 mg/Kg caused no significant reductions in HW (Table 5), BW (Table 5), and ECHO -derived ventricular structure (Figure 10A-D) or function (Figure 12A-D). However, the highest GDF11 dose tested (5 mg/Kg) in sham mice caused significant reductions in HW (Table 5), BW (Table 5), HW/TL (Figure 8C), ECHO -derived cardiac mass and dimensions (Figure 10C,D), and

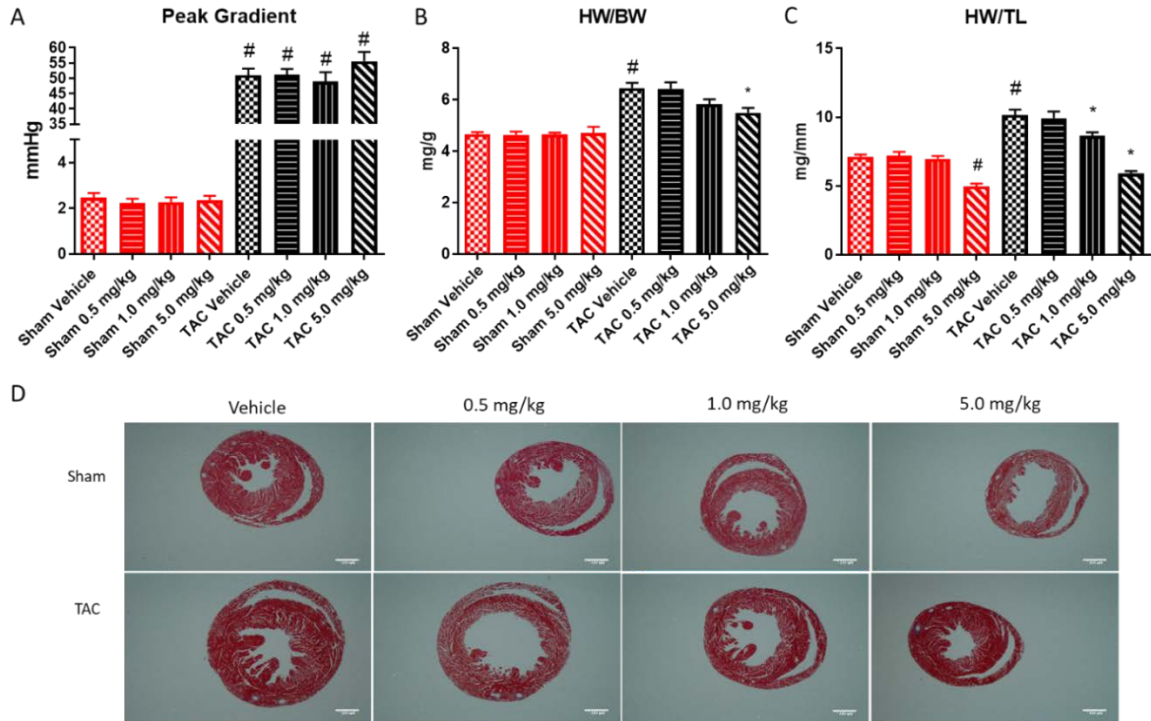


Figure 8. GDF11 reduces TAC-induced cardiac hypertrophy. A: Peak pressure gradients across the aortic constriction were measured 1 week after TAC or sham surgery. B,C: Heart weight to body weight ratio and heart weight to tibia length ratio were determined 21 days after TAC surgery (16/17 days after TAC surgery for mice treated with 5.0 mg/kg). D: Representative images of the mid-papillary transverse sections of hearts after 21 days of TAC and 14 injections of GDF11 or vehicle (16/17 days after TAC surgery and 9 or 10 injections for mice treated with 5.0 mg/kg of GDF11). Data are represented as mean \pm SEM. * $p < 0.05$ vs vehicle-treated TAC mice. # $p < 0.05$ vs vehicle-treated sham mice.

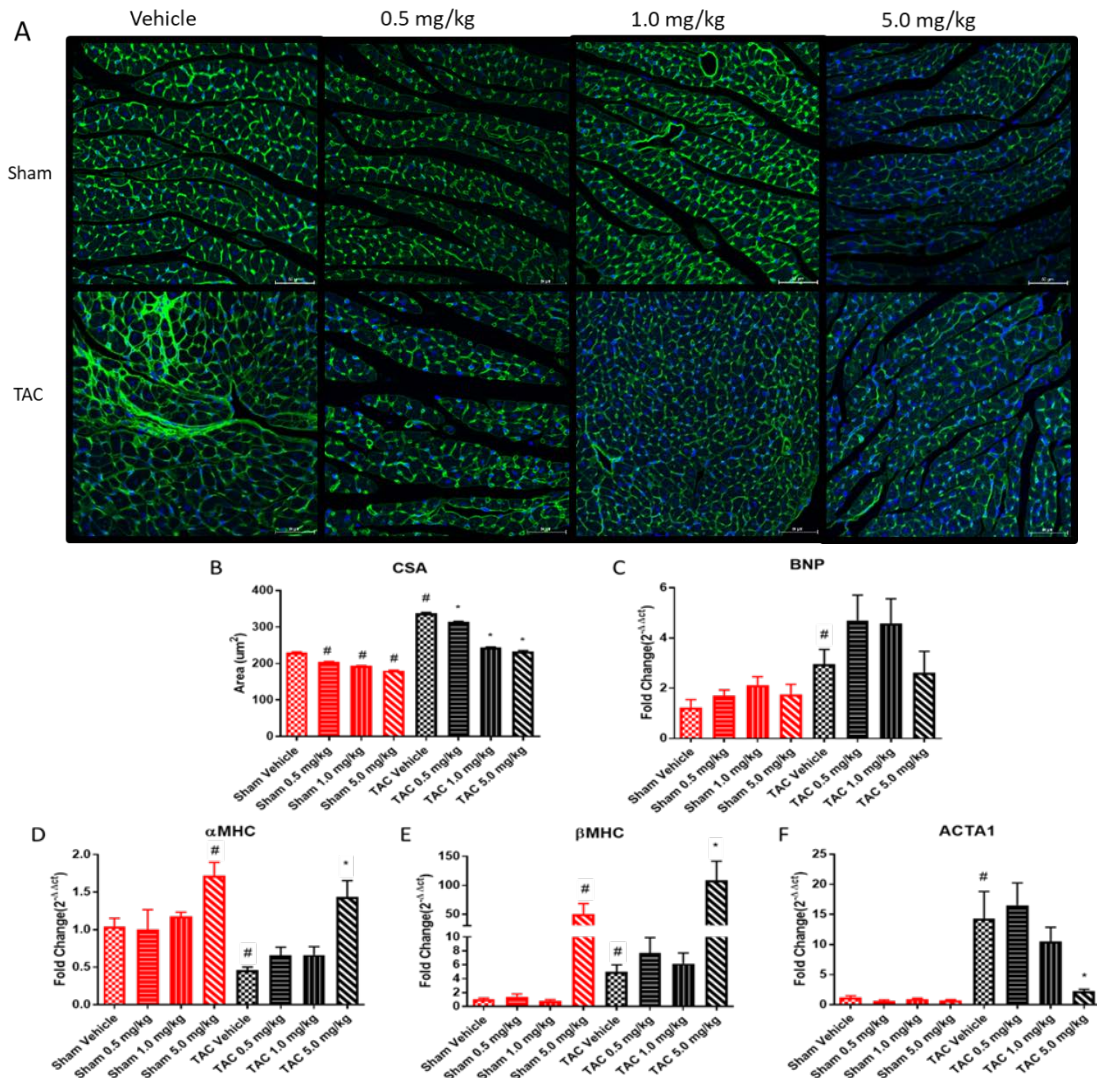


Figure 9. GDF11 decreases myocyte cross-sectional area and alters expression of markers of hypertrophy. A: Representative images of wheat germ agglutinin staining. B: Quantification of cross sectional areas of cardiac myocytes in WGA stained hearts from 3-8 mice per group. At least 300 myocytes with nuclei were analyzed per mouse. Scale bar = 50 microns. C-F: RT-PCR analysis of BNP, alpha skeletal actin (Acta1), alpha myosin heavy chain (α MHC) and beta myosin heavy chain (β MHC) mRNA expression. All data are represented as mean \pm SEM * $p < 0.05$ vs vehicle-treated TAC mice. # $p < 0.05$ vs vehicle-treated sham mice.

Table 5. Terminal Weights. Heart weight, body weight, tibia length, and lung weights were measured at time of sacrifice 14 days post initial injection of GDF11 (9 or 10 injections for mice treated with 5.0 mg/kg of GDF11). * $p < 0.05$ vs vehicle-treated TAC mice. # $p < 0.05$ vs vehicle-treated sham mice.

	BW (g)	HW (mg)	TL (mm)	HW/BW (mg/g)	HW/TL (mg/mm)	LW/BW (mg/g)
Sham Vehicle	26.53±1.60	123.80±9.81	17.37±0.44	4.42±0.30	6.80±0.58	4.95±0.28
Sham 0.5mg/kg	26.98±2.34	125.65±17.39	17.43±0.32	4.65±0.44	7.21±0.98	5.35±0.50
Sham 1.0 mg/kg	25.56±1.94	119.34±12.84	17.11±0.21	4.66±0.24	6.98±0.77	5.53±0.37
Sham 5.0 mg/kg	18.73±1.74#	87.61±10.71#	17.63±0.58	4.71±0.70	4.97±0.56#	7.07±0.66#
TAC Vehicle	27.04±2.21	175.09±29.64#	17.21±0.38	6.47±0.88#	10.17±1.66#	5.51±0.49
TAC 0.5 mg/kg	26.73±1.97	172.74±34.97	17.39±0.32	6.44±1.04	9.94±2.00	5.85±1.50
TAC 1.0 mg/kg	25.94±2.28	150.83±17.84*	17.47±0.48	5.84±0.76	8.64±1.07*	5.91±1.65
TAC 5.0 mg/kg	18.92±0.95*	103.88±11.76*	17.63±0.38	5.50±0.65*	5.89±0.65*	6.83±0.39*

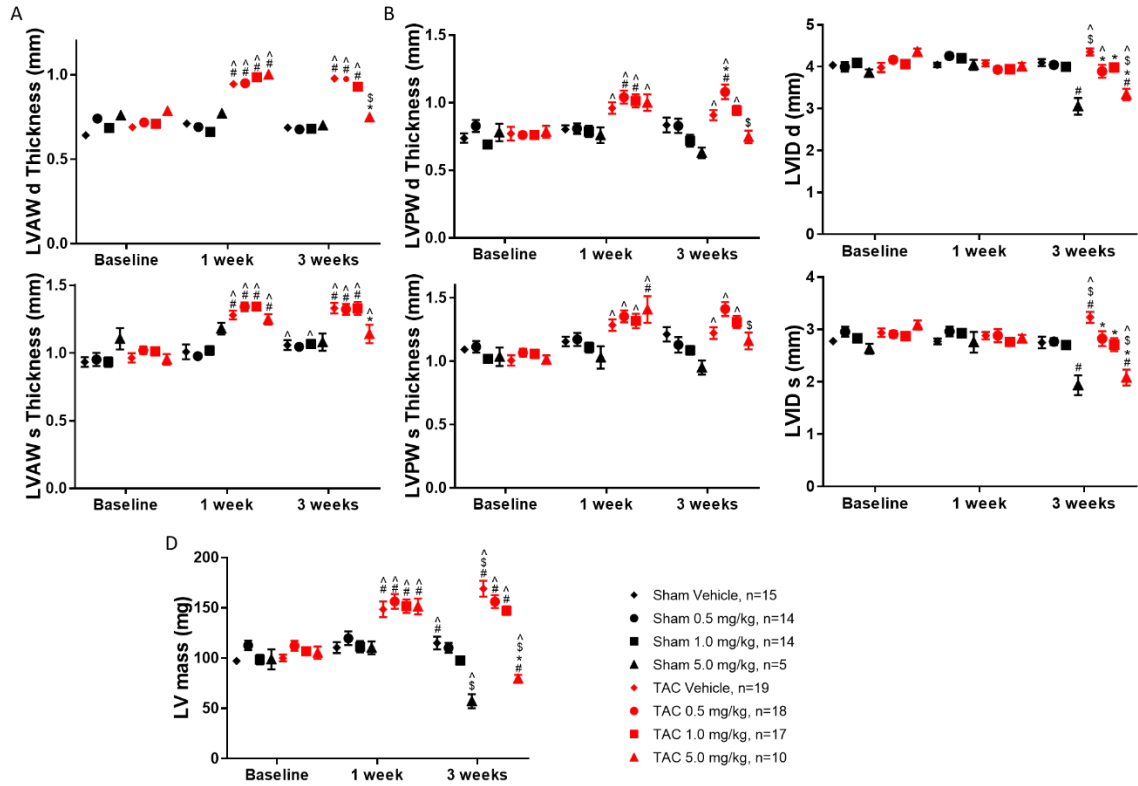


Figure 10. GDF11 altered cardiac remodeling after TAC. Echocardiography was performed at baseline, 1, and 3 weeks after TAC surgery. A: Left ventricular anterior wall thickness (top: diastole bottom: systole) B: Left ventricular posterior wall thickness C: Left ventricular internal dimension (top: diastole, bottom: systole). D: Left ventricular mass. Data are represented as mean \pm SEM * $p < 0.05$ vs vehicle-treated TAC mice at same time point. # $p < 0.05$ vs vehicle-treated sham mice at same time point. ^ $p < 0.05$ vs same group at baseline. \$ $p < 0.05$ vs same group at 1 week.

myocyte CSA (Figure 9B). There was no significant effect of 5 mg/Kg GDF11 on HW/BW in sham mice (Figure 8B). GDF11 caused small but significant reductions in myocyte CSA at all doses tested in sham mice (Figure 9B). Sham mice treated with 5 mg/Kg GDF11 showed signs of severe cachexia (see below) and either died or had to be euthanized 10-11 days after GDF11 treatment.

In TAC mice, the lowest GDF11 dose (0.5 mg/Kg) had no significant effect on BW, HW and ECHO-derived ventricular structure or mass. The 1.0 mg/Kg GDF11 dose caused a significant reduction in HW and HW/TL (Table 5, Figure 8C). The highest GDF11 dose (5 mg/Kg) caused significant reductions in HW (Table 5), BW (Table 5), HW/TL (Figure 8C), and ECHO-derived LV wall thicknesses, dimensions, and cardiac mass (Figure 10A-D). GDF11 cause significant reductions in myocyte CSA in TAC mice with CSA regressing to almost normal levels at 1 mg/Kg, a dose that did not induce severe cachexia (Figure 9B). GDF11 decreased some hypertrophy markers in TAC mice (Figure 9C-F), but the 5 mg/Kg dose had complex effects in both sham and TAC mice, with some hypertrophy markers decreasing while others increased. Like sham mice, TAC mice treated with 5 mg/Kg GDF11 showed signs of severe cachexia, were lethargic and needed to be euthanized 9-10 days after treatment was initiated.

These findings suggest that GDF11 induces a dose-dependent decrease in pathological cardiac hypertrophy, but also induces a body wasting phenotype (see below) that can become so severe at high GDF11 doses (5.0 mg/kg) that mice either died or had to be euthanized because they lost in excess of 30% of their body weight within 9-10 days of treatment (Figure 11).

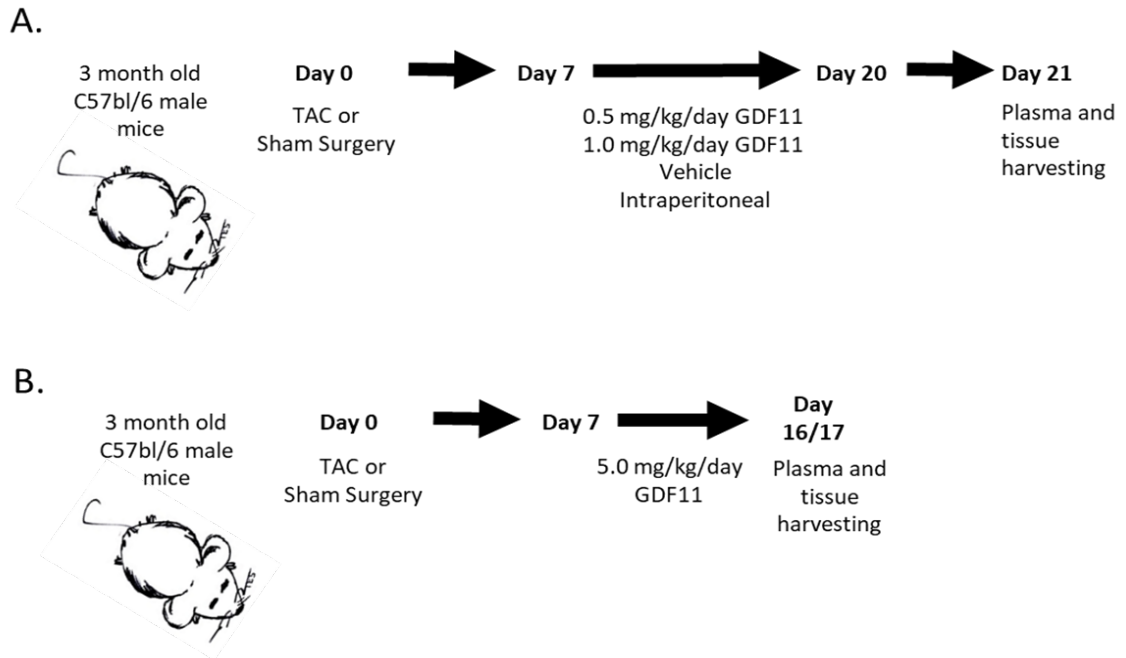


Figure 11. Schematic of experimental protocol. A: 12-13-week-old mice underwent TAC surgery. Mice were treated with vehicle or GDF11 at a dose 0.5mg/kg/day or 1.0 mg/kg/day via an IP injection for 14 days. Mice were euthanized after 21 days of TAC and tissue and plasma were collected. B: Mice receiving the 5.0 mg/kg/day dose of GDF11 had to be euthanized after 9 or 10 days of treatment with GDF11. Tissue and plasma were collected on day 16 or 17 of TAC.

GDF11 Improves Cardiac Function.

ECHO was used to determine time dependent changes in cardiac structure and function in sham and TAC mice treated with vehicle or GDF11 one week after surgery. In vehicle treated TAC mice, the ventricle began to dilate and pump function began to decline by week 3 post TAC with significant decreases in ejection fraction and fractional shortening and an increase in end-systolic and end-diastolic LV volumes (Figure 12A-C). TAC mice treated with the 0.5 mg/kg of GDF11 experienced similar decreases in ejection fraction and fractional shortening (Figure 12A,B). However, TAC mice treated with 1.0 mg/kg of GDF11 exhibited a modest increase in ejection fraction and fractional shortening and dilation was not present. 5.0 mg/kg of GDF11 caused a significant increase in ejection fraction and fractional shortening in TAC mice between weeks 1 and 3 post-TAC (Figure 12A,B). Sham mice treated with the 5.0 mg/kg dose also experienced an increase in EF, but this was not significant. End systolic and end diastolic volumes were unchanged in the 0.5 and 1.0 mg/kg treated TAC mice between weeks 1 and 3 post-TAC, while these volumes significantly decreased in the 5.0 mg/kg treated sham and TAC mice (Figure 12C,D). These results suggest that GDF11 treatment in TAC mice can prevent cardiac dilation and progressive depression of cardiac pump function.

GDF11 Decreased Cardiac Fibrosis.

Pathological cardiac hypertrophy induced by pressure overload is associated with increased cardiac fibrosis (Cingolani et al., 2004; Heymans et al., 2005; Ying et al., 2009). In the present experiments, TAC increased both perivascular and interstitial cardiac fibrosis in vehicle-treated TAC versus sham mice (Figure 13A-C). GDF11 treatment of sham mice had no effect on the amount of observed cardiac fibrosis, even at high GDF11 doses. In

TAC mice, all doses of GDF11 caused significant decreases in interstitial fibrosis but had no significant effect on perivascular fibrosis (Figure 13A-C). RT-PCR analysis of Collagen, type I, alpha 1 (Colla1) showed a significant increase in Colla1 mRNA abundance after TAC and a dose dependent reduction in Colla1 abundance in GDF11-treated TAC mice (Figure 13D).

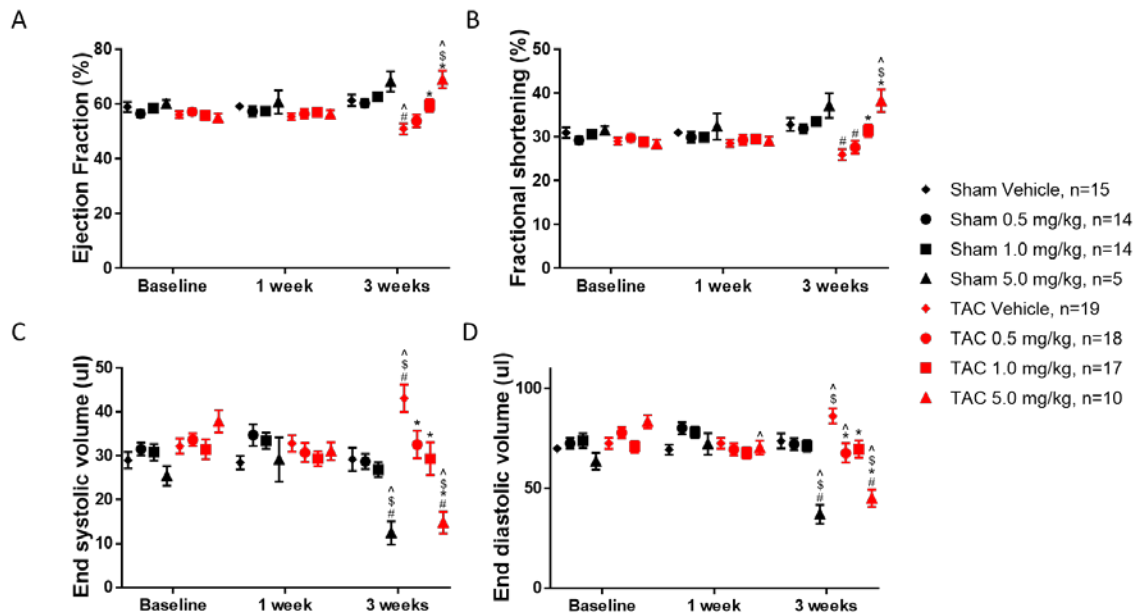


Figure 12. GDF11 improves cardiac function after TAC. Echocardiography was performed at baseline, 1, and 3 weeks after TAC surgery. A: Ejection fraction B: Fractional shortening. C: End systolic volume. D: End diastolic volume. Data are represented as mean \pm SEM *p<0.05 vs vehicle-treated TAC mice at same time point. #p<0.05 vs vehicle-treated sham mice at same time point. ^<0.05 vs same group at baseline. \$p<0.05 vs same group at 1 week.

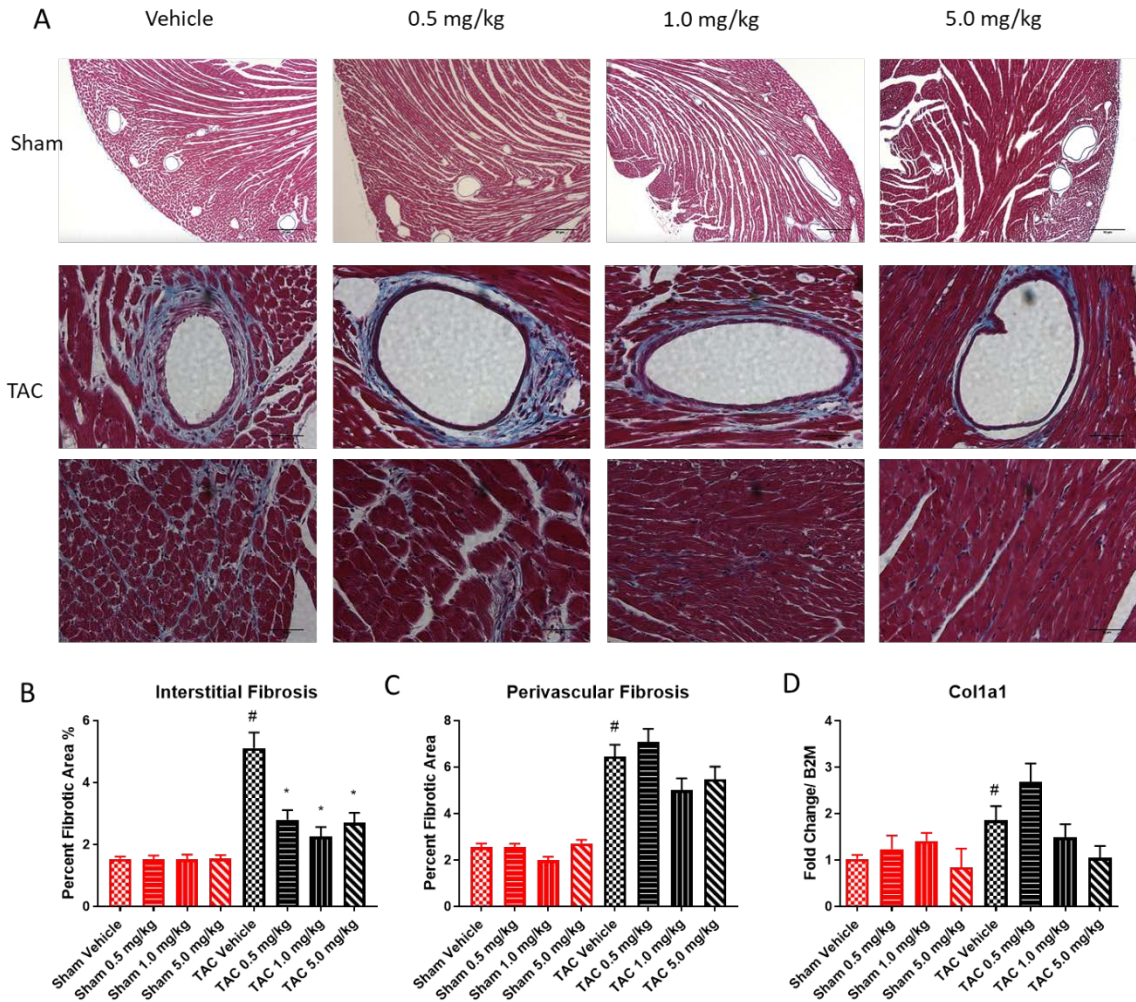


Figure 13. GDF11 reduces interstitial fibrosis and collagen mRNA expression. GDF11 treatment began 1 week after mice underwent TAC surgery. A: Representative images of hearts stained with Masson's trichrome. B: Quantification of interstitial fibrosis from Masson's trichrome staining. C: Quantification of fibrosis from areas containing vessels. D: RT-PCR analysis of collagen1a1 (col1a1) mRNA expression. Data are represented as mean \pm SEM * $p < 0.05$ vs vehicle-treated TAC mice. # $p < 0.05$ vs vehicle-treated sham mice

High doses of GDF11 cause cachexia:

Both sham and TAC mice receiving a 5.0 mg/kg dose of GDF11 lost approximately 30 percent of their body weight within 9 days of treatment compared to 5% for mice receiving the 1.0 mg/kg dose and a weight gain of about 1% for vehicle treated TAC mice (Figure 14A, Table 6). Three weeks of pressure overload had no effect on BW or skeletal muscle (Figure 14E-H) and organ weights (Figure 14B-D). Treatment with 0.5 mg/kg and 1.0 mg/kg of GDF11 also had no effect on the weight of these tissues. However, sham and TAC mice treated with the 5.0 mg/kg dose of GDF11 had decreased tibialis anterior, quadriceps, triceps, and gastrocnemius weights, as well as decreases in liver, kidney and spleen weights (Figure 14B-H). Lung weight was unaffected (Table 5). These results show that high doses of GDF11 cause severe body wasting and can cause death.

Table 6. Body weights and percent body weight change. Body weights were measured prior to the first injection and at sacrifice. Data are represented as mean \pm SEM * $p < 0.05$ vs vehicle-treated TAC mice. # $p < 0.05$ vs vehicle-treated sham mice.

	BW day 1	BW at sacrifice	Percent BW change
Sham Vehicle	26.89 \pm 1.55	26.53 \pm 1.60	-1.28 \pm 3.15
Sham 0.5mg/kg	28.49 \pm 2.28	26.98 \pm 2.34	-5.32 \pm 2.70#
Sham 1mg/kg	26.88 \pm 1.94	25.56 \pm 1.94	-4.90 \pm 2.43#
Sham 5.0 mg/kg	27.41 \pm 2.34	18.73 \pm 1.74#	-31.52 \pm 5.87#
TAC Vehicle	26.79 \pm 1.96	27.04 \pm 2.21	0.88 \pm 3.05
TAC 0.5 mg/kg	28.30 \pm 2.02	26.73 \pm 1.97	-5.38 \pm 4.83*
TAC 1.0 mg/kg	28.01 \pm 1.98	25.94 \pm 2.28	-7.24 \pm 7.41*
TAC 5.0 mg/kg	28.34 \pm 1.76	18.92 \pm 0.95*	-32.86 \pm 4.95*

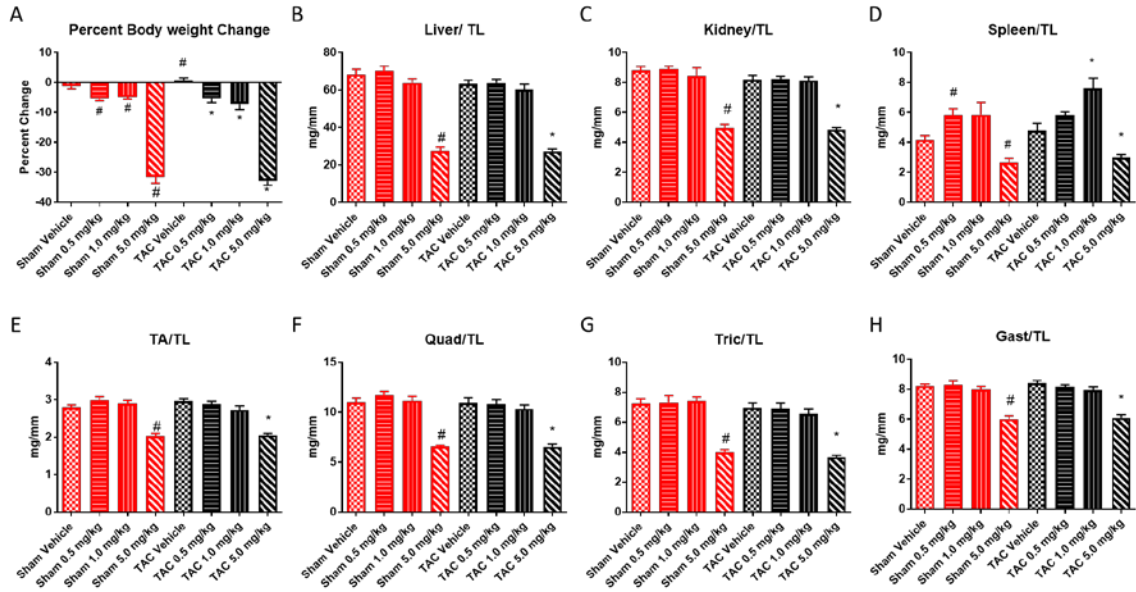


Figure 14. GDF11 induces severe cachexia at high dosage. Mice were weighed daily beginning with the first dose of GDF11. A: percent body weight change was calculated using the weight at time of sacrifice and the weight at the time of the first injection of GDF11. B-D: Liver weight to tibia length, kidney weight to tibia length, and spleen weight to tibia length ratios were analyzed 21 days after TAC surgery (16/17 days after TAC surgery and 9 for mice treated with 5.0 mg/kg of GDF11). E-F: Tibialis anterior (TA) weight to tibia length, Quadriceps (Quad) weight to tibia length, triceps (Tric) weight to tibia length, and gastrocnemius (Gast) weight to tibia length ratios were analyzed 21 days after TAC surgery (16/17 days after TAC surgery and 9 for mice treated with 5.0 mg/kg of GDF11). Data are represented as mean \pm SEM * $p < 0.05$ vs vehicle-treated TAC mice. # $p < 0.05$ vs vehicle-treated sham mice.

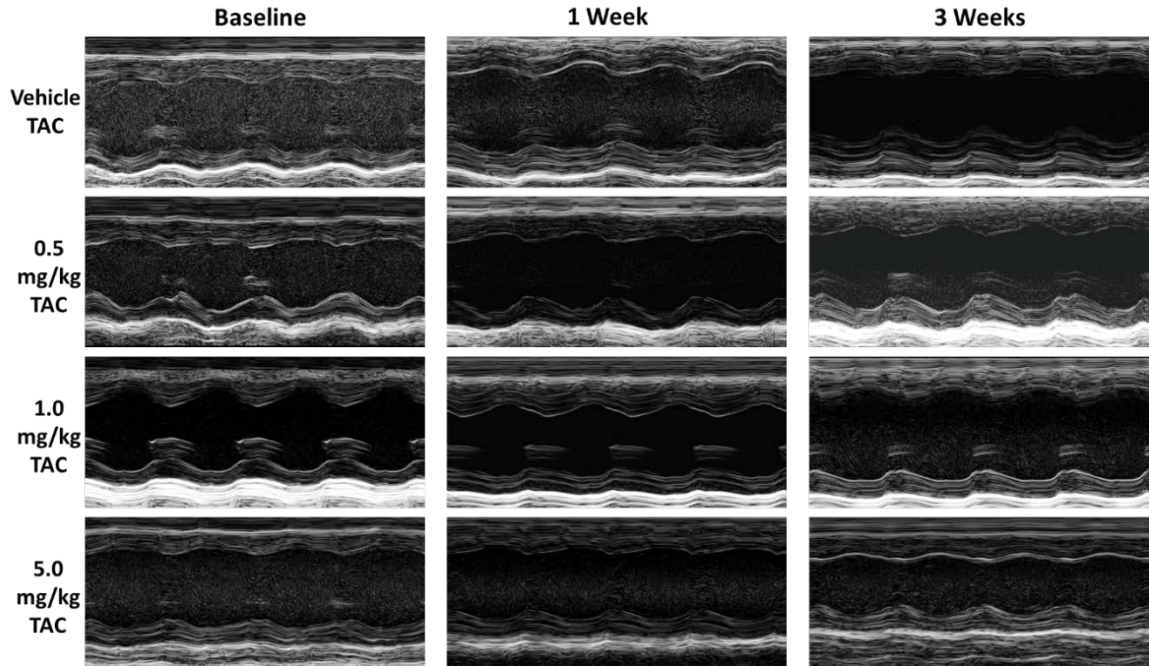


Figure 15. Representative M-mode echocardiograms. Echocardiograms are shown for TAC animals in each treatment group at the three measured time points: baseline, 1 week and 3 weeks after TAC surgery. Each set of images follows a single animal.

Discussion

Pathological cardiac hypertrophy (PCH) is a consequence of multiple cardiovascular diseases and is a major cause of morbidity and mortality (Ho et al., 1998). There is an unmet clinical need for novel therapeutic strategies to reduce PCH and thereby improve the quality and duration of patients' lives. Recent studies have suggested that GDF11 is a natural, circulating, anti-PCH factor. GDF11 levels in the blood may decrease with aging and this decrease has been associated with the emergence of pathological hypertrophy (Loffredo et al., 2013). A single study suggests that restoring normal GDF11

levels in old mice reverses PCH (Loffredo et al., 2013), consistent with a natural anti-hypertrophic effect. However, the beneficial effects of GDF11 in old mice have not been routinely confirmed (Smith et al., 2015) and there is evidence that excess GDF11 levels have severe adverse effects that would obviously limit its usefulness as a therapeutic.

The purpose of this study was to determine dose dependent effects of circulating recombinant GDF11 on cardiac structure and function in normal healthy mice as well as in mice with PCH induced by transverse aortic constriction (TAC). A dose ranging study was performed because the literature suggests that much of the current controversy regarding possible beneficial or adverse GDF11 effects result from different GDF11 dosing (Walker et al., 2017), poorly characterized recombinant GDF11 (Poggioli et al., 2016) and the difficulty in reliably measuring blood levels of biologically active GDF11 (Jamaiyar et al., 2017; Schafer et al., 2016). In this regard it was previously suggested that a GDF11 treatment dose of 0.1mg/kg per day was sufficient to reverse aging induced PCH but had no effect on TAC- induced PCH (Loffredo et al., 2013). Our group was unable to confirm that old mice actually had any PCH and we could not find any PCH reversal with this GDF11 dose (0.1 mg/kg) (Smith et al., 2015). In subsequent studies, others showed that GDF11 doses of 0.5 mg/kg and 1.0 mg/kg reduced HW/BW ratios in normal young and aged mice as well as myocyte cross sectional area (Poggioli et al., 2016), suggestive of a body wasting phenotype. A major goal of the present study was to determine if an anti-PCH effect of GDF11 could be separated from its ability to cause skeletal muscle wasting (Hammers et al., 2017; Zimmers et al., 2017).

GDF11 Reduces PCH and Improves Cardiac Structure and Function.

In the present study, PCH induced by TAC was produced in normal young mice. After PCH was confirmed (one week after surgical induction), mice were then randomized to different treatment groups for a dose ranging study in which mice were treated with intraperitoneal injections of GDF11 (0.5, 1.0 and 5.0 mg/kg/day) or vehicle for up to 14 days. At the completion of the study, we tested the plasma for increases in the circulating concentration of GDF11 and the heart for evidence of Smad2 phosphorylation. These experiments showed that daily injections of GDF11 increased the circulating blood concentrations of GDF11 and activated the canonical GDF11 signaling pathway in the heart (Figure 7B,C).

A previous study showed that 10 IP injections of GDF11 at 1.0 mg/kg caused a decrease in both HW/BW ratio and myocyte cross sectional area (CSA) in non-injured young and old mice (Poggioli et al., 2016). These findings suggest that GDF11 might reduce cardiac size but the cause is not entirely clear. Our study showed small but significant reductions in myocyte CSA at all GDF11 doses in sham mice. However, our findings differ from previous published results in that treatment of normal animals with 0.5 mg/kg and 1.0 mg/kg of GDF11 had no significant effect on their HW, BW, HW/BW or HW/TL ratios. There were small reductions in HW and BW at these doses but they were not significantly different than in untreated animals. However, the highest GDF11 dose (5 mg/Kg) tested indeed caused profound reductions in both body and heart weight but again, there was not a significant reduction in HW/BW. The fact that HW/BW changes were not induced in normal (sham) animals suggests to us that the primary dose dependent effect of

GDF11 was to reduce lean body mass, and heart size was then reduced as a function of its changing work demands.

In mice with TAC induced PCH, GDF11 caused a decrease in HW/BW and HW/TL at both the 1.0 mg/kg and 5.0 mg/kg doses. However, only the 5.0 mg/Kg GDF11 dose caused a significant reduction in BW with lethargy and overall body wasting (see below). A significant dose dependent decrease in the myocyte cross sectional area was observed in TAC mice treated with GDF11, and a dose dependent decrease in the LV mass was also observed in the GDF11 treated TAC mice.

A previous report suggested that GDF11 does not reduce TAC induced hypertrophy (Loffredo et al., 2013). This study (Loffredo et al., 2013) used a very low GDF11 dose of 0.1 mg/kg/day and did not test a range of GDF11 levels. We found clear evidence that GDF11 can cause dose-dependent reductions in PCH. Our studies employed a range of GDF11 doses that went from low doses that cause little or no changes in normal or TAC-induced cardiac structure and function to high doses that caused severe cachexia and premature death. Within this dosing range (1 mg/Kg) we observed reductions in TAC-induced cardiac (and cardiac myocyte) size without major changes in BW. The broad range of GDF11 doses we used could explain the differences between ours and other related GDF11 studies. Overall, we observed potentially beneficial anti-hypertrophic effects that were best observed at our 1.0 mg/kg/day dose of GDF11. Larger effects were seen at our highest dose (5 mg/Kg/day) but interpretation of these effects is complicated by the severe cachexia that was also observed. The reduction in HW/BW toward sham levels that was caused by GDF11 suggests to us that it can blunt pathological cardiac hypertrophy.

The highest GDF11 dose tested (5 mg/kg/day) caused severe muscle (and other organ/tissue) wasting (more than a 30% loss of BW in 9 days) in both normal and TAC mice that caused death or severe lethargy that forced us to euthanize the mice. In the TAC mice, the 5.0 mg/Kg treatment caused significant reductions in LV wall thicknesses and internal dimensions compared to the vehicle treated TAC mice, with the walls returning to baseline thickness and the LVID decreasing.

GDF11 treatment of TAC mice increased cardiac systolic function, as measured by ECHO, and reduced dysfunctional ventricular remodeling (ventricular dilation). This result supports some but conflicts with other studies (Zimmers et al., 2017) that have reported that mice injected with GDF11 secreting CHO cells had reduced cardiac size, but also reduced systolic function (Zimmers et al., 2017). In our experiments, ECHO derived systolic function decreased significantly between baseline and 3 weeks in vehicle treated TAC mice and the LV chamber began to dilate (Figure 10C), consistent with the time dependent changes in cardiac structure and function that are a prelude to heart failure in this animal model (G. Li et al., 2017; Schipke et al., 2016). A major finding of the present study is that GDF11 treatment prevented or reversed these structural and functional changes (Figures 10A-D, 12A-D), albeit over a narrow dosing range. Collectively, these results suggest that there is a rGDF11 dose range that can reverse the progression of PCH and improve cardiac function without causing cachexia.

GDF11 Reduces TAC-Induced Interstitial Fibrosis.

TAC induced significant increases in cardiac interstitial and perivascular fibrosis (Figure 13A,B). This has been shown in many previous studies (Cates et al., 2018; Furihata et al., 2016; Hirose et al., 2017; Ying et al., 2009; Zhao et al., 2018). Members of the TGF β

family of proteins are thought to be involved in pathological cardiac fibrosis (Bieseemann et al., 2015; Koitabashi et al., 2011; Shimano et al., 2011). Unexpectedly, we found a rGDF11 dependent decrease in interstitial fibrosis in the TAC mice (Figure 13A,B). This effect was observed at all GDF11 doses tested. The basis for this antifibrotic effect of GDF11 is unclear and likely involves multiple factors including direct effects on myocytes and fibroblasts (Brown, Ambler, Mitchell, & Long, 2005) as well as potential modulation of the immune cells that invade hearts with PCH (Ying et al., 2009).

High GDF11 Treatment Doses Cause Cachexia and Death.

The primary goal of our study was to test potential anti-PCH effects of circulating GDF11. We used recombinant GDF11 to explore this idea. The most common method for treatment with rGDF11 is daily intraperitoneal injections (Du et al., 2017; Egerman et al., 2015; Katsimpardi et al., 2014; Loffredo et al., 2013; Poggioli et al., 2016; Sinha et al., 2014; Smith et al., 2015). This method delivers GDF11 into the systemic circulation and allows for effects on tissues other than the heart. At the lowest doses used, 0.5 and 1.0 mg/kg/day, we saw no apparent negative noncardiac effects of GDF11 in either sham or TAC mice (Figure 14 B-H). However, mice treated with the highest dose tested, 5.0 mg/kg, experienced severe cachexia and had to be sacrificed within 10 days of treatment due to severe weight loss and lethargy in every treated mouse and the death of a few mice. The cachexic effects of GDF11 have been reported previously (Hammers et al., 2017; Zimmers et al., 2017) and were not surprising. GDF11 is highly homologous to another TGF β family member, myostatin. Myostatin activates the canonical SMAD2/3 pathway to negatively regulate skeletal muscle growth (McPherron et al., 1997; Trendelenburg et al., 2009). The cachexia seen in our study at high GDF11 doses is likely due to mechanisms recently defined

by others (Jones et al., 2018). Our results clearly show that high levels of circulating GDF11 mimic the skeletal muscle atrophy effects of high levels of myostatin.

Our study documents what appears to be beneficial dose dependent GDF11 effects on PCH and cardiac fibrosis. One caution is comparing our dosing with that in other studies (Egerman et al., 2015; Katsimpardi et al., 2014; Loffredo et al., 2013; Poggioli et al., 2016; Sinha et al., 2014). Differences in bioactivity of the rGDF11 used could make these comparisons dangerous. It was for this reason that we used a broad range of rGDF11 doses. The results of the experiments with this approach support the idea that increasing circulating GDF11 levels can reduce PCH, improve cardiac structure and function, and reduce pressure overload induced cardiac fibrosis. However, the clinical usefulness of this strategy is likely limited by the fact that the dose range for the cachexic effects of rGDF11 likely overlaps with those of its antihypertrophic effects. These issues would need to be resolved in future studies.

CHAPTER 4

CONCLUSIONS AND FUTURE DIRECTIONS

PCH usually results from diseases such as chronic hypertension, ischemic heart disease or from genetic defects (Bernardo et al., 2010; Frey & Olson, 2003; Orenstein et al., 1995; Richard, Villard, Charron, & Isnard, 2006; Tanijiri, 1975). PCH characteristics include increased HW/BW, increased cardiomyocyte size, altered myocyte Ca^{2+} handling properties, decreased cardiomyocyte number due to myocyte death, and increased fibrosis (Bernardo et al., 2010; McMullen & Jennings, 2007). Some of these features can be present in the aged heart (Lakatta & Levy, 2003b), but there is little conclusive evidence that PCH develops as part of the normal aging process. In fact, age-related cardiomyopathy is often secondary to the acquisition of cardiovascular disease (Bujak et al., 2008; Olivetti et al., 1991). Molecular causes of true age-dependent cardiomyopathy, in the absence of disease, are not well defined. There is a need for studies that better explain the mechanisms of aging-related cardiomyopathy to better define strategies to prevent or reverse these defects. This knowledge gap has led to studies that explore true age dependent changes in cardiac structure and function versus disease dependent changes in these parameters. One idea for age dependent cardiac changes is that circulating factors that determine them are altered with age. GDF11 has been explored as one of these factors.

The role of TGF- β family members in cardiovascular disease has been investigated. TGF- β family members are known to negatively regulate muscle, but studies involving GDF11 have produced conflicting results regarding its role in cardiac muscle. GDF11 is highly homologous to another TGF- β family member, GDF8 (myostatin) which has been studied more extensively in the heart and in skeletal muscle.

Recently, in a controversial study from the laboratories of Richard Lee and Amy Wagers, GDF11 was shown to regulate age-related cardiac hypertrophy. Healthy, disease free, aged mice were thought to have PCH when compared to young 8-week-old animals, and this was thought to be correlated with a decreased level of circulating GDF11. The authors suggested that GDF11 levels in the blood decreased with aging and daily injections of GDF11 (0.1 mg/kg) for 30 days reversed PCH in aged mice (Loffredo et al., 2013). However, these data could not be confirmed in our studies. Using the same dose, we found that daily injections of GDF11 had no effect on cardiac structure or function in the same strain of mice. We also were unable to determine the native levels of GDF11 in mice because the levels were too low to accurately detect with the methods available to us. In addition, the original data that involved parabiosis were suspect since the decrease in cardiac weight was proportional to the large reductions in BW that occurred in old mice conjoined to young mice.

Our findings do not support the hypotheses that 1) there is PCH in old C57Bl6 mice, 2) that reduced circulating levels of GDF11 are responsible for this PCH and 3) that raising GDF11 levels with daily injections of rGDF11 rescues cardiac pathologies (because none could be shown). Additional work with carefully characterized animal models and rGDF11 should help the field determine if raising circulating GDF11 levels in old age repairs or damages the heart. These studies should focus on a range of doses rather than a single low dose to determine if there is a therapeutic range for GDF11.

Our dose response study in young healthy mice and in mice after TAC surgery was designed to answer two questions: 1) whether GDF11 can have beneficial effects on the heart under stress, and 2) what are the effects of GDF11 on the normal heart? The ability

of GDF11 to regulate muscle mass has been established; increased amounts of circulating GDF11 can lead to both skeletal and cardiac muscle wasting (Hammers et al., 2017; Zimmers et al., 2017). Although these studies showed that overexpression of GDF11 via AAV-2 or CHO cells resulted in decreases in cardiac and skeletal muscle mass and function as well as death of mice at high doses, other studies have shown modest changes in cardiac mass with no effect on skeletal mass, or even beneficial effects of GDF11 treatment on the heart (Poglioli 2015, Du 2017).

Our data show an effect of GDF11 on the heart in both TAC and sham animals. Most molecular changes occur within the first few days of pressure overload. At the three-week time point used in this study, we were unable to see any differences in phosphorylation levels of key proteins involved in the common signaling pathways activated during hypertrophy. It is also important to note that although we see preservation of cardiac function in the 1.0mg/kg group at 3 weeks post TAC, and we begin to see a decline of function in the vehicle treated animals, it is unclear whether this dose would be able to prevent the transition of these mice to heart failure over time.

Further studies are needed at earlier time points to assess changes in the signaling pathways that lead to the induction of hypertrophy, and at longer time points to assess the preservation of function. Another dose ranging study with doses between 1.0 mg/kg and 5.0 mg/kg would help to determine a true therapeutic range for systemic increases in circulating GDF11, as we see some beneficial effects of GDF11 on hypertrophy at 1 mg/kg with no obvious changes in skeletal muscle mass, while the highest dose used (5.0 mg/kg) resulted in cachexia and death within 10 days. Targeted delivery of GDF11 to the heart after TAC should also be investigated to determine if GDF11 could be beneficial to the

heart without the negative effects on skeletal muscle or other organs. We also observed an anti-fibrotic effect in our GDF11 treatment groups after TAC. The canonical signaling pathway for GDF11 activates Smad2/3 which are known to be involved in promoting fibrosis (Khalil et al., 2017). The root of this anti-fibrotic effect in vivo needs to be investigated.

REFERENCES CITED

- Agrawal, R., Agrawal, N., Koyani, C. N., & Singh, R. (2010). Molecular targets and regulators of cardiac hypertrophy. *Pharmacol Res*, *61*(4), 269-280. doi:10.1016/j.phrs.2009.11.012
- Angelov, S. N., Hu, J. H., Wei, H., Airhart, N., Shi, M., & Dichek, D. A. (2017). TGF-beta (Transforming Growth Factor-beta) Signaling Protects the Thoracic and Abdominal Aorta From Angiotensin II-Induced Pathology by Distinct Mechanisms. *Arterioscler Thromb Vasc Biol*, *37*(11), 2102-2113. doi:10.1161/ATVBAHA.117.309401
- Artaza, J. N., Reisz-Porszasz, S., Dow, J. S., Kloner, R. A., Tsao, J., Bhasin, S., & Gonzalez-Cadavid, N. F. (2007). Alterations in myostatin expression are associated with changes in cardiac left ventricular mass but not ejection fraction in the mouse. *J Endocrinol*, *194*(1), 63-76. doi:10.1677/JOE-07-0072
- Attisano, L., & Wrana, J. L. (2002). Signal transduction by the TGF-beta superfamily. *Science*, *296*(5573), 1646-1647. doi:10.1126/science.1071809
- Bae, S., Yalamarti, B., Ke, Q., Choudhury, S., Yu, H., Karumanchi, S. A., . . . Kang, P. M. (2011). Preventing progression of cardiac hypertrophy and development of heart failure by paricalcitol therapy in rats. *Cardiovasc Res*, *91*(4), 632-639. doi:10.1093/cvr/cvr133
- Balakumar, P., & Jagadeesh, G. (2010). Multifarious molecular signaling cascades of cardiac hypertrophy: can the muddy waters be cleared? *Pharmacol Res*, *62*(5), 365-383. doi:10.1016/j.phrs.2010.07.003
- Barouch, L. A., Cappola, T. P., Harrison, R. W., Crone, J. K., Rodriguez, E. R., Burnett, A. L., & Hare, J. M. (2003). Combined loss of neuronal and endothelial nitric oxide synthase causes premature mortality and age-related hypertrophic cardiac remodeling in mice. *J Mol Cell Cardiol*, *35*(6), 637-644.

- Barrick, C. J., Dong, A., Waikel, R., Corn, D., Yang, F., Threadgill, D. W., & Smyth, S. S. (2009). Parent-of-origin effects on cardiac response to pressure overload in mice. *Am J Physiol Heart Circ Physiol*, 297(3), H1003-1009. doi:10.1152/ajpheart.00896.2008
- Barry, S. P., Davidson, S. M., & Townsend, P. A. (2008). Molecular regulation of cardiac hypertrophy. *Int J Biochem Cell Biol*, 40(10), 2023-2039. doi:10.1016/j.biocel.2008.02.020
- Benjamin, E. J., Blaha, M. J., Chiuve, S. E., Cushman, M., Das, S. R., Deo, R., . . . Stroke Statistics, S. (2017). Heart Disease and Stroke Statistics-2017 Update: A Report From the American Heart Association. *Circulation*, 135(10), e146-e603. doi:10.1161/CIR.0000000000000485
- Berk, B. C., Fujiwara, K., & Lehoux, S. (2007). ECM remodeling in hypertensive heart disease. *J Clin Invest*, 117(3), 568-575. doi:10.1172/JCI31044
- Bernardo, B. C., Weeks, K. L., Pretorius, L., & McMullen, J. R. (2010). Molecular distinction between physiological and pathological cardiac hypertrophy: experimental findings and therapeutic strategies. *Pharmacol Ther*, 128(1), 191-227. doi:10.1016/j.pharmthera.2010.04.005
- Biesemann, N., Mendler, L., Kostin, S., Wietelmann, A., Borchardt, T., & Braun, T. (2015). Myostatin induces interstitial fibrosis in the heart via TAK1 and p38. *Cell Tissue Res*. doi:10.1007/s00441-015-2139-2
- Biesemann, N., Mendler, L., Wietelmann, A., Hermann, S., Schafers, M., Kruger, M., . . . Braun, T. (2014). Myostatin regulates energy homeostasis in the heart and prevents heart failure. *Circ Res*, 115(2), 296-310. doi:10.1161/CIRCRESAHA.115.304185
- Bish, L. T., Morine, K. J., Sleeper, M. M., & Sweeney, H. L. (2010). Myostatin is upregulated following stress in an Erk-dependent manner and negatively regulates cardiomyocyte

growth in culture and in a mouse model. *PLoS One*, 5(4), e10230.

doi:10.1371/journal.pone.0010230

Boengler, K., Schulz, R., & Heusch, G. (2009). Loss of cardioprotection with ageing. *Cardiovasc Res*, 83(2), 247-261. doi:10.1093/cvr/cvp033

Bourajjaj, M., Armand, A. S., da Costa Martins, P. A., Weijts, B., van der Nagel, R., Heeneman, S., . . . De Windt, L. J. (2008). NFATc2 is a necessary mediator of calcineurin-dependent cardiac hypertrophy and heart failure. *J Biol Chem*, 283(32), 22295-22303.

doi:10.1074/jbc.M801296200

Brand, T., & Schneider, M. D. (1995). The TGF beta superfamily in myocardium: ligands, receptors, transduction, and function. *J Mol Cell Cardiol*, 27(1), 5-18.

Braz, J. C., Gregory, K., Pathak, A., Zhao, W., Sahin, B., Klevitsky, R., . . . Molkenin, J. D. (2004). PKC-alpha regulates cardiac contractility and propensity toward heart failure. *Nat Med*, 10(3), 248-254. doi:10.1038/nm1000

Breitbart, A., Auger-Messier, M., Molkenin, J. D., & Heineke, J. (2011). Myostatin from the heart: local and systemic actions in cardiac failure and muscle wasting. *Am J Physiol Heart Circ Physiol*, 300(6), H1973-1982. doi:10.1152/ajpheart.00200.2011

Brown, R. D., Ambler, S. K., Mitchell, M. D., & Long, C. S. (2005). The cardiac fibroblast: therapeutic target in myocardial remodeling and failure. *Annu Rev Pharmacol Toxicol*, 45, 657-687. doi:10.1146/annurev.pharmtox.45.120403.095802

Brun, C. E., & Rudnicki, M. A. (2015). GDF11 and the Mythical Fountain of Youth. *Cell Metab*, 22(1), 54-56. doi:10.1016/j.cmet.2015.05.009

Bueno, O. F., De Windt, L. J., Tymitz, K. M., Witt, S. A., Kimball, T. R., Klevitsky, R., . . . Molkenin, J. D. (2000). The MEK1-ERK1/2 signaling pathway promotes compensated cardiac

hypertrophy in transgenic mice. *EMBO J*, 19(23), 6341-6350.

doi:10.1093/emboj/19.23.6341

Bujak, M., & Frangogiannis, N. G. (2007). The role of TGF-beta signaling in myocardial infarction and cardiac remodeling. *Cardiovasc Res*, 74(2), 184-195.

doi:10.1016/j.cardiores.2006.10.002

Bujak, M., Kweon, H. J., Chatila, K., Li, N., Taffet, G., & Frangogiannis, N. G. (2008). Aging-related defects are associated with adverse cardiac remodeling in a mouse model of reperfused myocardial infarction. *J Am Coll Cardiol*, 51(14), 1384-1392.

doi:10.1016/j.jacc.2008.01.011

Castillero, E., Akashi, H., Wang, C., Najjar, M., Ji, R., Kennel, P. J., . . . George, I. (2015). Cardiac myostatin upregulation occurs immediately after myocardial ischemia and is involved in skeletal muscle activation of atrophy. *Biochem Biophys Res Commun*, 457(1), 106-111.

doi:10.1016/j.bbrc.2014.12.057

Cates, C., Rousselle, T., Wang, J., Quan, N., Wang, L., Chen, X., . . . Li, J. (2018). Activated protein C protects against pressure overload-induced hypertrophy through AMPK signaling.

Biochem Biophys Res Commun, 495(4), 2584-2594. doi:10.1016/j.bbrc.2017.12.125

Chen, W. Y., Hong, J., Gannon, J., Kakkar, R., & Lee, R. T. (2015). Myocardial pressure overload induces systemic inflammation through endothelial cell IL-33. *Proc Natl Acad Sci U S A*,

112(23), 7249-7254. doi:10.1073/pnas.1424236112

Cingolani, O. H., Yang, X. P., Liu, Y. H., Villanueva, M., Rhaleb, N. E., & Carretero, O. A. (2004).

Reduction of cardiac fibrosis decreases systolic performance without affecting diastolic function in hypertensive rats. *Hypertension*, 43(5), 1067-1073.

doi:10.1161/01.HYP.0000125013.22494.c5

- Cohn, R. D., Liang, H. Y., Shetty, R., Abraham, T., & Wagner, K. R. (2007). Myostatin does not regulate cardiac hypertrophy or fibrosis. *Neuromuscul Disord*, *17*(4), 290-296.
doi:10.1016/j.nmd.2007.01.011
- Conboy, I. M., Conboy, M. J., Wagers, A. J., Girma, E. R., Weissman, I. L., & Rando, T. A. (2005). Rejuvenation of aged progenitor cells by exposure to a young systemic environment. *Nature*, *433*(7027), 760-764. doi:10.1038/nature03260
- Cowan, B. R., & Young, A. A. (2009). Left ventricular hypertrophy and renin-angiotensin system blockade. *Curr Hypertens Rep*, *11*(3), 167-172.
- Diez, J., Lopez, B., Gonzalez, A., & Querejeta, R. (2001). Clinical aspects of hypertensive myocardial fibrosis. *Curr Opin Cardiol*, *16*(6), 328-335.
- Divakaran, V., Adroge, J., Ishiyama, M., Entman, M. L., Haudek, S., Sivasubramanian, N., & Mann, D. L. (2009). Adaptive and maladaptive effects of SMAD3 signaling in the adult heart after hemodynamic pressure overloading. *Circ Heart Fail*, *2*(6), 633-642.
doi:10.1161/CIRCHEARTFAILURE.108.823070
- Drazner, M. H. (2011). The progression of hypertensive heart disease. *Circulation*, *123*(3), 327-334. doi:10.1161/CIRCULATIONAHA.108.845792
- Du, G. Q., Shao, Z. B., Wu, J., Yin, W. J., Li, S. H., Wu, J., . . . Li, R. K. (2017). Targeted myocardial delivery of GDF11 gene rejuvenates the aged mouse heart and enhances myocardial regeneration after ischemia-reperfusion injury. *Basic Res Cardiol*, *112*(1), 7.
doi:10.1007/s00395-016-0593-y
- Duran, J. M., Makarewich, C. A., Sharp, T. E., Starosta, T., Zhu, F., Hoffman, N. E., . . . Houser, S. R. (2013). Bone-derived stem cells repair the heart after myocardial infarction through

transdifferentiation and paracrine signaling mechanisms. *Circ Res*, 113(5), 539-552.

doi:10.1161/CIRCRESAHA.113.301202

Duran, J. M., Taghavi, S., Berretta, R. M., Makarewich, C. A., Sharp Iii, T., Starosta, T., . . . Houser, S. R. (2012). A characterization and targeting of the infarct border zone in a swine model of myocardial infarction. *Clin Transl Sci*, 5(5), 416-421. doi:10.1111/j.1752-8062.2012.00432.x

Edgley, A. J., Krum, H., & Kelly, D. J. (2012). Targeting fibrosis for the treatment of heart failure: a role for transforming growth factor-beta. *Cardiovasc Ther*, 30(1), e30-40.

doi:10.1111/j.1755-5922.2010.00228.x

Egerman, M. A., Cadena, S. M., Gilbert, J. A., Meyer, A., Nelson, H. N., Swalley, S. E., . . . Glass, D. J. (2015). GDF11 Increases with Age and Inhibits Skeletal Muscle Regeneration. *Cell Metab*. doi:10.1016/j.cmet.2015.05.010

doi:10.1016/j.cmet.2015.05.010

Ernsberger, P., Koletsky, R. J., Baskin, J. S., & Collins, L. A. (1996). Consequences of weight cycling in obese spontaneously hypertensive rats. *Am J Physiol*, 270(4 Pt 2), R864-872.

Esposito, G., Rapacciuolo, A., Naga Prasad, S. V., Takaoka, H., Thomas, S. A., Koch, W. J., & Rockman, H. A. (2002). Genetic alterations that inhibit in vivo pressure-overload hypertrophy prevent cardiac dysfunction despite increased wall stress. *Circulation*, 105(1), 85-92.

Fernandez-Sola, J., Borrissier-Pairo, F., Antunez, E., & Tobias, E. (2015). Myostatin and insulin-like growth factor-1 in hypertensive heart disease: a prospective study in human heart donors. *J Hypertens*, 33(4), 851-858; discussion 859.

doi:10.1097/HJH.0000000000000493

Francis, G. S. (2001). Pathophysiology of chronic heart failure. *Am J Med*, 110 Suppl 7A, 37S-46S.

- Freeman, G. L., Harris, M. M., Ghidoni, J. J., Page, A., Cantu, T. L., & Young, E. (1994). Analysis of myocardial response to significant weight loss in obese rats. *Am J Clin Nutr*, *59*(3), 566-571.
- Frey, N., Katus, H. A., Olson, E. N., & Hill, J. A. (2004). Hypertrophy of the heart: a new therapeutic target? *Circulation*, *109*(13), 1580-1589.
doi:10.1161/01.CIR.0000120390.68287.BB
- Frey, N., & Olson, E. N. (2003). Cardiac hypertrophy: the good, the bad, and the ugly. *Annu Rev Physiol*, *65*, 45-79. doi:10.1146/annurev.physiol.65.092101.142243
- Furihata, T., Kinugawa, S., Takada, S., Fukushima, A., Takahashi, M., Homma, T., . . . Tsutsui, H. (2016). The experimental model of transition from compensated cardiac hypertrophy to failure created by transverse aortic constriction in mice. *Int J Cardiol Heart Vasc*, *11*, 24-28. doi:10.1016/j.ijcha.2016.03.007
- Gaudin, C., Ishikawa, Y., Wight, D. C., Mahdavi, V., Nadal-Ginard, B., Wagner, T. E., . . . Homcy, C. J. (1995). Overexpression of Gs alpha protein in the hearts of transgenic mice. *J Clin Invest*, *95*(4), 1676-1683. doi:10.1172/JCI117843
- George, I., Bish, L. T., Kamalakkannan, G., Petrilli, C. M., Oz, M. C., Naka, Y., . . . Maybaum, S. (2010). Myostatin activation in patients with advanced heart failure and after mechanical unloading. *Eur J Heart Fail*, *12*(5), 444-453. doi:10.1093/eurjhf/hfq039
- Goldspink, D. F., Burniston, J. G., & Tan, L. B. (2003). Cardiomyocyte death and the ageing and failing heart. *Exp Physiol*, *88*(3), 447-458.
- Grossman, W., Jones, D., & McLaurin, L. P. (1975). Wall stress and patterns of hypertrophy in the human left ventricle. *J Clin Invest*, *56*(1), 56-64. doi:10.1172/JCI108079

- Haider, A. W., Larson, M. G., Benjamin, E. J., & Levy, D. (1998). Increased left ventricular mass and hypertrophy are associated with increased risk for sudden death. *J Am Coll Cardiol*, 32(5), 1454-1459.
- Haldeman, G. A., Croft, J. B., Giles, W. H., & Rashidee, A. (1999). Hospitalization of patients with heart failure: National Hospital Discharge Survey, 1985 to 1995. *Am Heart J*, 137(2), 352-360. doi:10.1053/hj.1999.v137.95495
- Hammers, D. W., Merscham-Banda, M., Hsiao, J. Y., Engst, S., Hartman, J. J., & Sweeney, H. L. (2017). Supraphysiological levels of GDF11 induce striated muscle atrophy. *EMBO Mol Med*, 9(4), 531-544. doi:10.15252/emmm.201607231
- Hata, A., & Chen, Y. G. (2016). TGF-beta Signaling from Receptors to Smads. *Cold Spring Harb Perspect Biol*, 8(9). doi:10.1101/cshperspect.a022061
- Heidenreich, P. A., Trogdon, J. G., Khavjou, O. A., Butler, J., Dracup, K., Ezekowitz, M. D., . . . Outcomes, R. (2011). Forecasting the future of cardiovascular disease in the United States: a policy statement from the American Heart Association. *Circulation*, 123(8), 933-944. doi:10.1161/CIR.0b013e31820a55f5
- Heineke, J., Auger-Messier, M., Xu, J., Sargent, M., York, A., Welle, S., & Molkenin, J. D. (2010). Genetic deletion of myostatin from the heart prevents skeletal muscle atrophy in heart failure. *Circulation*, 121(3), 419-425. doi:10.1161/CIRCULATIONAHA.109.882068
- Heineke, J., & Molkenin, J. D. (2006). Regulation of cardiac hypertrophy by intracellular signalling pathways. *Nat Rev Mol Cell Biol*, 7(8), 589-600. doi:10.1038/nrm1983
- Helms, S. A., Azhar, G., Zuo, C., Theus, S. A., Bartke, A., & Wei, J. Y. (2010). Smaller cardiac cell size and reduced extra-cellular collagen might be beneficial for hearts of Ames dwarf mice. *Int J Biol Sci*, 6(5), 475-490.

- Heymans, S., Schroen, B., Vermeersch, P., Milting, H., Gao, F., Kassner, A., . . . Janssens, S. (2005). Increased cardiac expression of tissue inhibitor of metalloproteinase-1 and tissue inhibitor of metalloproteinase-2 is related to cardiac fibrosis and dysfunction in the chronic pressure-overloaded human heart. *Circulation*, *112*(8), 1136-1144. doi:10.1161/CIRCULATIONAHA.104.516963
- Hirose, M., Takano, H., Hasegawa, H., Tadokoro, H., Hashimoto, N., Takemura, G., & Kobayashi, Y. (2017). The effects of dipeptidyl peptidase-4 on cardiac fibrosis in pressure overload-induced heart failure. *J Pharmacol Sci*, *135*(4), 164-173. doi:10.1016/j.jphs.2017.11.006
- Ho, Y. L., Wu, C. C., Lin, L. C., Huang, C. H., Chen, W. J., Chen, M. F., . . . Lee, Y. T. (1998). Assessment of the coronary artery disease and systolic dysfunction in hypertensive patients with the dobutamine-atropine stress echocardiography: effect of the left ventricular hypertrophy. *Cardiology*, *89*(1), 52-58.
- Iwase, M., Bishop, S. P., Uechi, M., Vatner, D. E., Shannon, R. P., Kudej, R. K., . . . Vatner, S. F. (1996). Adverse effects of chronic endogenous sympathetic drive induced by cardiac GS alpha overexpression. *Circ Res*, *78*(4), 517-524.
- Jackson, M. F., Luong, D., Vang, D. D., Garikipati, D. K., Stanton, J. B., Nelson, O. L., & Rodgers, B. D. (2012). The aging myostatin null phenotype: reduced adiposity, cardiac hypertrophy, enhanced cardiac stress response, and sexual dimorphism. *J Endocrinol*, *213*(3), 263-275. doi:10.1530/JOE-11-0455
- Jamaiyar, A., Wan, W., Janota, D. M., Enrick, M. K., Chilian, W. M., & Yin, L. (2017). The versatility and paradox of GDF 11. *Pharmacol Ther*, *175*, 28-34. doi:10.1016/j.pharmthera.2017.02.032

- Jones, J. E., Cadena, S. M., Gong C., Wang X., Chen Z., Wang S.X., . . . Glass, D. J. (2018).
Supraphysiologic Administration of GDF11 Induces Cachexia in Part by Upregulating
GDF15. *Cell Reports*, 22(6), 1522-1530.
- Joseph, P., Leong, D., McKee, M., Anand, S. S., Schwalm, J. D., Teo, K., . . . Yusuf, S. (2017).
Reducing the Global Burden of Cardiovascular Disease, Part 1: The Epidemiology and
Risk Factors. *Circ Res*, 121(6), 677-694. doi:10.1161/CIRCRESAHA.117.308903
- Kai, H., Mori, T., Tokuda, K., Takayama, N., Tahara, N., Takemiya, K., . . . Imaizumi, T. (2006).
Pressure overload-induced transient oxidative stress mediates perivascular
inflammation and cardiac fibrosis through angiotensin II. *Hypertens Res*, 29(9), 711-718.
doi:10.1291/hypres.29.711
- Kallikourdis, M., Martini, E., Carullo, P., Sardi, C., Roselli, G., Greco, C. M., . . . Condorelli, G.
(2017). T cell costimulation blockade blunts pressure overload-induced heart failure. *Nat
Commun*, 8, 14680. doi:10.1038/ncomms14680
- Kato, T., Niizuma, S., Inuzuka, Y., Kawashima, T., Okuda, J., Tamaki, Y., . . . Shioi, T. (2010).
Analysis of metabolic remodeling in compensated left ventricular hypertrophy and heart
failure. *Circ Heart Fail*, 3(3), 420-430. doi:10.1161/CIRCHEARTFAILURE.109.888479
- Katsimpardi, L., Litterman, N. K., Schein, P. A., Miller, C. M., Loffredo, F. S., Wojtkiewicz, G. R., . . .
Rubin, L. L. (2014). Vascular and neurogenic rejuvenation of the aging mouse brain by
young systemic factors. *Science*, 344(6184), 630-634. doi:10.1126/science.1251141
- Kearney, P. M., Whelton, M., Reynolds, K., Muntner, P., Whelton, P. K., & He, J. (2005). Global
burden of hypertension: analysis of worldwide data. *Lancet*, 365(9455), 217-223.
doi:10.1016/S0140-6736(05)17741-1

- Kehat, I., & Molkenin, J. D. (2010). Molecular pathways underlying cardiac remodeling during pathophysiological stimulation. *Circulation*, *122*(25), 2727-2735.
doi:10.1161/CIRCULATIONAHA.110.942268
- Khalil, H., Kanisicak, O., Prasad, V., Correll, R. N., Fu, X., Schips, T., . . . Molkenin, J. D. (2017). Fibroblast-specific TGF-beta-Smad2/3 signaling underlies cardiac fibrosis. *J Clin Invest*, *127*(10), 3770-3783. doi:10.1172/JCI94753
- Kiper, C., Grimes, B., Van Zant, G., & Satin, J. (2013). Mouse strain determines cardiac growth potential. *PLoS One*, *8*(8), e70512. doi:10.1371/journal.pone.0070512
- Koitabashi, N., Danner, T., Zaiman, A. L., Pinto, Y. M., Rowell, J., Mankowski, J., . . . Kass, D. A. (2011). Pivotal role of cardiomyocyte TGF-beta signaling in the murine pathological response to sustained pressure overload. *J Clin Invest*, *121*(6), 2301-2312.
doi:10.1172/JCI44824
- Kollias, H. D., & McDermott, J. C. (2008). Transforming growth factor-beta and myostatin signaling in skeletal muscle. *J Appl Physiol (1985)*, *104*(3), 579-587.
doi:10.1152/jappphysiol.01091.2007
- Lakatta, E. G. (2015). So! What's aging? Is cardiovascular aging a disease? *J Mol Cell Cardiol*, *83*, 1-13. doi:10.1016/j.yjmcc.2015.04.005
- Lakatta, E. G., & Levy, D. (2003a). Arterial and cardiac aging: major shareholders in cardiovascular disease enterprises: Part I: aging arteries: a "set up" for vascular disease. *Circulation*, *107*(1), 139-146.
- Lakatta, E. G., & Levy, D. (2003b). Arterial and cardiac aging: major shareholders in cardiovascular disease enterprises: Part II: the aging heart in health: links to heart disease. *Circulation*, *107*(2), 346-354.

- Li, G., Xie, J., Chen, J., Li, R., Wu, H., Zhang, X., . . . Xu, B. (2017). Syndecan-4 deficiency accelerates the transition from compensated hypertrophy to heart failure following pressure overload. *Cardiovasc Pathol*, *28*, 74-79. doi:10.1016/j.carpath.2017.03.008
- Li, L., Zhou, N., Gong, H., Wu, J., Lin, L., Komuro, I., . . . Zou, Y. (2010). Comparison of angiotensin II type 1-receptor blockers to regress pressure overload-induced cardiac hypertrophy in mice. *Hypertens Res*, *33*(12), 1289-1297. doi:10.1038/hr.2010.182
- Li, X. M., Ma, Y. T., Yang, Y. N., Liu, F., Chen, B. D., Han, W., . . . Gao, X. M. (2009). Downregulation of survival signalling pathways and increased apoptosis in the transition of pressure overload-induced cardiac hypertrophy to heart failure. *Clin Exp Pharmacol Physiol*, *36*(11), 1054-1061. doi:10.1111/j.1440-1681.2009.05243.x
- Lijnen, P., & Petrov, V. (1999). Renin-angiotensin system, hypertrophy and gene expression in cardiac myocytes. *J Mol Cell Cardiol*, *31*(5), 949-970. doi:10.1006/jmcc.1999.0934
- Lijnen, P. J., Petrov, V. V., & Fagard, R. H. (2000). Induction of cardiac fibrosis by transforming growth factor-beta(1). *Mol Genet Metab*, *71*(1-2), 418-435. doi:10.1006/mgme.2000.3032
- Lim, H. W., De Windt, L. J., Steinberg, L., Taigen, T., Witt, S. A., Kimball, T. R., & Molkentin, J. D. (2000). Calcineurin expression, activation, and function in cardiac pressure-overload hypertrophy. *Circulation*, *101*(20), 2431-2437.
- Lips, D. J., Bueno, O. F., Wilkins, B. J., Purcell, N. H., Kaiser, R. A., Lorenz, J. N., . . . Molkentin, J. D. (2004). MEK1-ERK2 signaling pathway protects myocardium from ischemic injury in vivo. *Circulation*, *109*(16), 1938-1941. doi:10.1161/01.CIR.0000127126.73759.23

- Lips, D. J., deWindt, L. J., van Kraaij, D. J., & Doevendans, P. A. (2003). Molecular determinants of myocardial hypertrophy and failure: alternative pathways for beneficial and maladaptive hypertrophy. *Eur Heart J*, *24*(10), 883-896.
- Loffredo, F. S., Steinhauser, M. L., Jay, S. M., Gannon, J., Pancoast, J. R., Yalamanchi, P., . . . Lee, R. T. (2013). Growth differentiation factor 11 is a circulating factor that reverses age-related cardiac hypertrophy. *Cell*, *153*(4), 828-839. doi:10.1016/j.cell.2013.04.015
- Luedde, M., Katus, H. A., & Frey, N. (2006). Novel molecular targets in the treatment of cardiac hypertrophy. *Recent Pat Cardiovasc Drug Discov*, *1*(1), 1-20.
- Malek, M. (1999). Health economics of heart failure. *Heart*, *82 Suppl 4*, IV11-13.
- Massague, J. (1990). The transforming growth factor-beta family. *Annu Rev Cell Biol*, *6*, 597-641. doi:10.1146/annurev.cb.06.110190.003121
- McMullen, J. R., & Jennings, G. L. (2007). Differences between pathological and physiological cardiac hypertrophy: novel therapeutic strategies to treat heart failure. *Clin Exp Pharmacol Physiol*, *34*(4), 255-262. doi:10.1111/j.1440-1681.2007.04585.x
- McPherron, A. C. (2010). Metabolic Functions of Myostatin and Gdf11. *Immunol Endocr Metab Agents Med Chem*, *10*(4), 217-231. doi:10.2174/187152210793663810
- McPherron, A. C., Lawler, A. M., & Lee, S. J. (1997). Regulation of skeletal muscle mass in mice by a new TGF-beta superfamily member. *Nature*, *387*(6628), 83-90. doi:10.1038/387083a0
- Meguro, T., Hong, C., Asai, K., Takagi, G., McKinsey, T. A., Olson, E. N., & Vatner, S. F. (1999). Cyclosporine attenuates pressure-overload hypertrophy in mice while enhancing susceptibility to decompensation and heart failure. *Circ Res*, *84*(6), 735-740.

- Mehta, P. K., & Griendling, K. K. (2007). Angiotensin II cell signaling: physiological and pathological effects in the cardiovascular system. *Am J Physiol Cell Physiol*, 292(1), C82-97. doi:10.1152/ajpcell.00287.2006
- Morissette, M. R., Cook, S. A., Foo, S., McKoy, G., Ashida, N., Novikov, M., . . . Rosenzweig, A. (2006). Myostatin regulates cardiomyocyte growth through modulation of Akt signaling. *Circ Res*, 99(1), 15-24. doi:10.1161/01.RES.0000231290.45676.d4
- Morissette, M. R., Stricker, J. C., Rosenberg, M. A., Buranasombati, C., Levitan, E. B., Mittleman, M. A., & Rosenzweig, A. (2009). Effects of myostatin deletion in aging mice. *Aging Cell*, 8(5), 573-583. doi:10.1111/j.1474-9726.2009.00508.x
- Mosher, D. S., Quignon, P., Bustamante, C. D., Sutter, N. B., Mellersh, C. S., Parker, H. G., & Ostrander, E. A. (2007). A mutation in the myostatin gene increases muscle mass and enhances racing performance in heterozygote dogs. *PLoS Genet*, 3(5), e79. doi:10.1371/journal.pgen.0030079
- Nadruz, W. (2015). Myocardial remodeling in hypertension. *J Hum Hypertens*, 29(1), 1-6. doi:10.1038/jhh.2014.36
- Ohsawa, Y., Okada, T., Nishimatsu, S., Ishizaki, M., Suga, T., Fujino, M., . . . Sunada, Y. (2012). An inhibitor of transforming growth factor beta type I receptor ameliorates muscle atrophy in a mouse model of caveolin 3-deficient muscular dystrophy. *Lab Invest*, 92(8), 1100-1114. doi:10.1038/labinvest.2012.78
- Oie, E., Bjornerheim, R., Clausen, O. P., & Attramadal, H. (2000). Cyclosporin A inhibits cardiac hypertrophy and enhances cardiac dysfunction during postinfarction failure in rats. *Am J Physiol Heart Circ Physiol*, 278(6), H2115-2123. doi:10.1152/ajpheart.2000.278.6.H2115

- Olivetti, G., Melissari, M., Capasso, J. M., & Anversa, P. (1991). Cardiomyopathy of the aging human heart. Myocyte loss and reactive cellular hypertrophy. *Circ Res*, *68*(6), 1560-1568.
- Ooi, J. Y., Bernardo, B. C., & McMullen, J. R. (2014). The therapeutic potential of miRNAs regulated in settings of physiological cardiac hypertrophy. *Future Med Chem*, *6*(2), 205-222. doi:10.4155/fmc.13.196
- Orenstein, T. L., Parker, T. G., Butany, J. W., Goodman, J. M., Dawood, F., Wen, W. H., . . . Liu, P. P. (1995). Favorable left ventricular remodeling following large myocardial infarction by exercise training. Effect on ventricular morphology and gene expression. *J Clin Invest*, *96*(2), 858-866. doi:10.1172/JCI118132
- Pandya, K., Kim, H. S., & Smithies, O. (2006). Fibrosis, not cell size, delineates beta-myosin heavy chain reexpression during cardiac hypertrophy and normal aging in vivo. *Proc Natl Acad Sci U S A*, *103*(45), 16864-16869. doi:10.1073/pnas.0607700103
- Pardali, E., & Ten Dijke, P. (2012). TGFbeta signaling and cardiovascular diseases. *Int J Biol Sci*, *8*(2), 195-213. doi:10.7150/ijbs.3805
- Parsons, S. A., Millay, D. P., Sargent, M. A., McNally, E. M., & Molkentin, J. D. (2006). Age-dependent effect of myostatin blockade on disease severity in a murine model of limb-girdle muscular dystrophy. *Am J Pathol*, *168*(6), 1975-1985. doi:10.2353/ajpath.2006.051316
- Poggioli, T., Vujic, A., Yang, P., Macias-Trevino, C., Uygur, A., Loffredo, F. S., . . . Lee, R. T. (2016). Circulating Growth Differentiation Factor 11/8 Levels Decline With Age. *Circ Res*, *118*(1), 29-37. doi:10.1161/CIRCRESAHA.115.307521

- Qin, W., Du, N., Zhang, L., Wu, X., Hu, Y., Li, X., . . . Du, Z. (2015). Genistein alleviates pressure overload-induced cardiac dysfunction and interstitial fibrosis in mice. *Br J Pharmacol*, 172(23), 5559-5572. doi:10.1111/bph.13002
- Richard, P., Villard, E., Charron, P., & Isnard, R. (2006). The genetic bases of cardiomyopathies. *Journal of the American College of Cardiology*, 48(9), A79-A89. doi:10.1016/j.jacc.2006.09.014
- Ritter, O., & Neyses, L. (2003). The molecular basis of myocardial hypertrophy and heart failure. *Trends Mol Med*, 9(7), 313-321.
- Rodgers, B. D., Interlichia, J. P., Garikipati, D. K., Mamidi, R., Chandra, M., Nelson, O. L., . . . Santana, L. F. (2009). Myostatin represses physiological hypertrophy of the heart and excitation-contraction coupling. *J Physiol*, 587(Pt 20), 4873-4886. doi:10.1113/jphysiol.2009.172544
- Roger, V. L. (2013). Epidemiology of heart failure. *Circ Res*, 113(6), 646-659. doi:10.1161/CIRCRESAHA.113.300268
- Roth, G. A., Forouzanfar, M. H., Moran, A. E., Barber, R., Nguyen, G., Feigin, V. L., . . . Murray, C. J. (2015). Demographic and epidemiologic drivers of global cardiovascular mortality. *N Engl J Med*, 372(14), 1333-1341. doi:10.1056/NEJMoa1406656
- Rothermel, B. A., Berenji, K., Tannous, P., Kutschke, W., Dey, A., Nolan, B., . . . Hill, J. A. (2005). Differential activation of stress-response signaling in load-induced cardiac hypertrophy and failure. *Physiol Genomics*, 23(1), 18-27. doi:10.1152/physiolgenomics.00061.2005
- Ruckh, J. M., Zhao, J. W., Shadrach, J. L., van Wijngaarden, P., Rao, T. N., Wagers, A. J., & Franklin, R. J. (2012). Rejuvenation of regeneration in the aging central nervous system. *Cell Stem Cell*, 10(1), 96-103. doi:10.1016/j.stem.2011.11.019

- Rumyantsev, P. P. (1977). Interrelations of the proliferation and differentiation processes during cardiac myogenesis and regeneration. *Int Rev Cytol*, *51*, 186-273.
- Ryu, Y., Jin, L., Kee, H. J., Piao, Z. H., Cho, J. Y., Kim, G. R., . . . Jeong, M. H. (2016). Gallic acid prevents isoproterenol-induced cardiac hypertrophy and fibrosis through regulation of JNK2 signaling and Smad3 binding activity. *Sci Rep*, *6*, 34790. doi:10.1038/srep34790
- Sako, D., Grinberg, A. V., Liu, J., Davies, M. V., Castonguay, R., Maniatis, S., . . . Kumar, R. (2010). Characterization of the ligand binding functionality of the extracellular domain of activin receptor type IIb. *J Biol Chem*, *285*(27), 21037-21048. doi:10.1074/jbc.M110.114959
- Salazar, N. C., Chen, J., & Rockman, H. A. (2007). Cardiac GPCRs: GPCR signaling in healthy and failing hearts. *Biochim Biophys Acta*, *1768*(4), 1006-1018.
doi:10.1016/j.bbamem.2007.02.010
- Savabi, F., & Kirsch, A. (1992). Diabetic type of cardiomyopathy in food-restricted rats. *Can J Physiol Pharmacol*, *70*(7), 1040-1047.
- Schafer, M. J., Atkinson, E. J., Vanderboom, P. M., Kotajarvi, B., White, T. A., Moore, M. M., . . . LeBrasseur, N. K. (2016). Quantification of GDF11 and Myostatin in Human Aging and Cardiovascular Disease. *Cell Metab*, *23*(6), 1207-1215. doi:10.1016/j.cmet.2016.05.023
- Schipke, J., Grimm, C., Arnstein, G., Kockskamper, J., Sedej, S., & Muhlfeld, C. (2016). Cardiomyocyte loss is not required for the progression of left ventricular hypertrophy induced by pressure overload in female mice. *J Anat*, *229*(1), 75-81.
doi:10.1111/joa.12463
- Schultz Jel, J., Witt, S. A., Glascock, B. J., Nieman, M. L., Reiser, P. J., Nix, S. L., . . . Doetschman, T. (2002). TGF-beta1 mediates the hypertrophic cardiomyocyte growth induced by angiotensin II. *J Clin Invest*, *109*(6), 787-796. doi:10.1172/JCI14190

- Sharma, M., Kambadur, R., Matthews, K. G., Somers, W. G., Devlin, G. P., Conaglen, J. V., . . . Bass, J. J. (1999). Myostatin, a transforming growth factor-beta superfamily member, is expressed in heart muscle and is upregulated in cardiomyocytes after infarct. *J Cell Physiol*, *180*(1), 1-9. doi:10.1002/(SICI)1097-4652(199907)180:1<1::AID-JCP1>3.0.CO;2-V
- Shimano, M., Ouchi, N., Nakamura, K., Oshima, Y., Higuchi, A., Pimentel, D. R., . . . Walsh, K. (2011). Cardiac myocyte-specific ablation of follistatin-like 3 attenuates stress-induced myocardial hypertrophy. *J Biol Chem*, *286*(11), 9840-9848. doi:10.1074/jbc.M110.197079
- Shimizu, I., & Minamino, T. (2016). Physiological and pathological cardiac hypertrophy. *J Mol Cell Cardiol*, *97*, 245-262. doi:10.1016/j.yjmcc.2016.06.001
- Sinha, M., Jang, Y. C., Oh, J., Khong, D., Wu, E. Y., Manohar, R., . . . Wagers, A. J. (2014). Restoring systemic GDF11 levels reverses age-related dysfunction in mouse skeletal muscle. *Science*, *344*(6184), 649-652. doi:10.1126/science.1251152
- Skavdahl, M., Steenbergen, C., Clark, J., Myers, P., Demianenko, T., Mao, L., . . . Murphy, E. (2005). Estrogen receptor-beta mediates male-female differences in the development of pressure overload hypertrophy. *Am J Physiol Heart Circ Physiol*, *288*(2), H469-476. doi:10.1152/ajpheart.00723.2004
- Smith, S. C., Zhang, X., Zhang, X., Gross, P., Starosta, T., Mohsin, S., . . . Houser, S. R. (2015). GDF11 Does Not Rescue Aging-Related Pathological Hypertrophy. *Circ Res*, *117*(11), 926-932. doi:10.1161/CIRCRESAHA.115.307527
- Soonpaa, M. H., & Field, L. J. (1997). Assessment of cardiomyocyte DNA synthesis in normal and injured adult mouse hearts. *Am J Physiol*, *272*(1 Pt 2), H220-226. doi:10.1152/ajpheart.1997.272.1.H220

- Taghavi, S., Duran, J. M., Berretta, R. M., Makarewich, C. A., Udeshi, F., Sharp, T. E., . . . George, J. C. (2012). Validation of transcatheter left ventricular electromechanical mapping for assessment of cardiac function and targeted transendocardial injection in a porcine ischemia-reperfusion model. *Am J Transl Res*, *4*(2), 240-246.
- Tanijiri, H. (1975). Cardiac hypertrophy in spontaneously hypertensive rats. *Jpn Heart J*, *16*(2), 174-188.
- Teiger, E., Than, V. D., Richard, L., Wisnewsky, C., Tea, B. S., Gaboury, L., . . . Hamet, P. (1996). Apoptosis in pressure overload-induced heart hypertrophy in the rat. *J Clin Invest*, *97*(12), 2891-2897. doi:10.1172/JCI118747
- Tilley, D. G. (2011). G protein-dependent and G protein-independent signaling pathways and their impact on cardiac function. *Circ Res*, *109*(2), 217-230. doi:10.1161/CIRCRESAHA.110.231225
- Trendelenburg, A. U., Meyer, A., Rohner, D., Boyle, J., Hatakeyama, S., & Glass, D. J. (2009). Myostatin reduces Akt/TORC1/p70S6K signaling, inhibiting myoblast differentiation and myotube size. *Am J Physiol Cell Physiol*, *296*(6), C1258-1270. doi:10.1152/ajpcell.00105.2009
- Tsui, H., Zi, M., Wang, S., Chowdhury, S. K., Prehar, S., Liang, Q., . . . Wang, X. (2015). Smad3 Couples Pak1 With the Antihypertrophic Pathway Through the E3 Ubiquitin Ligase, Fbxo32. *Hypertension*, *66*(6), 1176-1183. doi:10.1161/HYPERTENSIONAHA.115.06068
- van Berlo, J. H., Maillet, M., & Molkenin, J. D. (2013). Signaling effectors underlying pathologic growth and remodeling of the heart. *J Clin Invest*, *123*(1), 37-45. doi:10.1172/JCI62839
- van Oort, R. J., van Rooij, E., Bourajjaj, M., Schimmel, J., Jansen, M. A., van der Nagel, R., . . . De Windt, L. J. (2006). MEF2 activates a genetic program promoting chamber dilation and

- contractile dysfunction in calcineurin-induced heart failure. *Circulation*, 114(4), 298-308.
doi:10.1161/CIRCULATIONAHA.105.608968
- Vilar, J. M., Jansen, R., & Sander, C. (2006). Signal processing in the TGF-beta superfamily ligand-receptor network. *PLoS Comput Biol*, 2(1), e3. doi:10.1371/journal.pcbi.0020003
- Walker, R. G., Czepnik, M., Goebel, E. J., McCoy, J. C., Vujic, A., Cho, M., . . . Thompson, T. B. (2017). Structural basis for potency differences between GDF8 and GDF11. *BMC Biol*, 15(1), 19. doi:10.1186/s12915-017-0350-1
- Waller, B. F. (1988). The old-age heart: normal aging changes which can produce or mimic cardiac disease. *Clin Cardiol*, 11(8), 513-517.
- Weiss, A., & Attisano, L. (2013). The TGFbeta superfamily signaling pathway. *Wiley Interdiscip Rev Dev Biol*, 2(1), 47-63. doi:10.1002/wdev.86
- Wenzel, S., Taimor, G., Piper, H. M., & Schluter, K. D. (2001). Redox-sensitive intermediates mediate angiotensin II-induced p38 MAP kinase activation, AP-1 binding activity, and TGF-beta expression in adult ventricular cardiomyocytes. *FASEB J*, 15(12), 2291-2293. doi:10.1096/fj.00-0827fje
- Wilkins, B. J., Dai, Y. S., Bueno, O. F., Parsons, S. A., Xu, J., Plank, D. M., . . . Molkentin, J. D. (2004). Calcineurin/NFAT coupling participates in pathological, but not physiological, cardiac hypertrophy. *Circ Res*, 94(1), 110-118. doi:10.1161/01.RES.0000109415.17511.18
- Wrana, J. L. (2013). Signaling by the TGFbeta superfamily. *Cold Spring Harb Perspect Biol*, 5(10), a011197. doi:10.1101/cshperspect.a011197

- Xing, F., Tan, X., Zhang, P. J., Ma, J., Zhang, Y., Xu, P., & Xu, Y. (2007). Characterization of amphioxus GDF8/11 gene, an archetype of vertebrate MSTN and GDF11. *Dev Genes Evol*, 217(7), 549-554. doi:10.1007/s00427-007-0162-3
- Yang, X., Sreejayan, N., & Ren, J. (2005). Views from within and beyond: narratives of cardiac contractile dysfunction under senescence. *Endocrine*, 26(2), 127-137. doi:10.1385/ENDO:26:2:127
- Ying, X., Lee, K., Li, N., Corbett, D., Mendoza, L., & Frangogiannis, N. G. (2009). Characterization of the inflammatory and fibrotic response in a mouse model of cardiac pressure overload. *Histochem Cell Biol*, 131(4), 471-481. doi:10.1007/s00418-008-0541-5
- Zannad, F., Briancon, S., Juilliere, Y., Mertes, P. M., Villemot, J. P., Alla, F., & Virion, J. M. (1999). Incidence, clinical and etiologic features, and outcomes of advanced chronic heart failure: the EPICAL Study. *Epidemiologie de l'Insuffisance Cardiaque Avancee en Lorraine. J Am Coll Cardiol*, 33(3), 734-742.
- Zhang, H., Makarewich, C. A., Kubo, H., Wang, W., Duran, J. M., Li, Y., . . . Houser, S. R. (2012). Hyperphosphorylation of the cardiac ryanodine receptor at serine 2808 is not involved in cardiac dysfunction after myocardial infarction. *Circ Res*, 110(6), 831-840. doi:10.1161/CIRCRESAHA.111.255158
- Zhang, L., Jaswal, J. S., Ussher, J. R., Sankaralingam, S., Wagg, C., Zaugg, M., & Lopaschuk, G. D. (2013). Cardiac insulin-resistance and decreased mitochondrial energy production precede the development of systolic heart failure after pressure-overload hypertrophy. *Circ Heart Fail*, 6(5), 1039-1048. doi:10.1161/CIRCHEARTFAILURE.112.000228
- Zhang, T., Maier, L. S., Dalton, N. D., Miyamoto, S., Ross, J., Jr., Bers, D. M., & Brown, J. H. (2003). The deltaC isoform of CaMKII is activated in cardiac hypertrophy and induces dilated

cardiomyopathy and heart failure. *Circ Res*, 92(8), 912-919.

doi:10.1161/01.RES.0000069686.31472.C5

Zhang, X., Azhar, G., Furr, M. C., Zhong, Y., & Wei, J. Y. (2003). Model of functional cardiac aging: young adult mice with mild overexpression of serum response factor. *Am J Physiol Regul Integr Comp Physiol*, 285(3), R552-560. doi:10.1152/ajpregu.00631.2002

Zhao, R. R., Ackers-Johnson, M., Stenzig, J., Chen, C., Ding, T., Zhou, Y., . . . Foo, R. S. Y. (2018).

Targeting Chondroitin Sulfate Glycosaminoglycans to Treat Cardiac Fibrosis in

Pathological Remodeling. *Circulation*. doi:10.1161/CIRCULATIONAHA.117.030353

Zimmers, T. A., Jiang, Y., Wang, M., Liang, T. W., Rupert, J. E., Au, E. D., . . . Koniaris, L. G. (2017).

Exogenous GDF11 induces cardiac and skeletal muscle dysfunction and wasting. *Basic*

Res Cardiol, 112(4), 48. doi:10.1007/s00395-017-0639-9